

# **User's Guide**

## **QUASES-ARXPS** **Quantitative Analysis of Surfaces** **by Electron Spectroscopy**

**Version 1.1**

**Software Package for Quantitative XPS/AES of Surface  
Nano-Structures  
by Analysis of the variation of  
Peak Intensities with Emission Angle**

© 1994-2012 QUASES Tougaard ApS  
All rights reserved.  
QUASES-ARXPS Software is developed by:  
*T. S. Lassen and S. Tougaard*

**QUASES Tougaard ApS**  
**Ridderhatten 316**  
**DK-5230 Odense SO.**  
**Denmark.**

Internet: [www.quases.com](http://www.quases.com)

E-mail: [tougaard@quases.com](mailto:tougaard@quases.com)

# Contents

<b>Introduction</b>	<b>1</b>
Installing and Running QUASES-ARXPS	3
System requirements	3
Installing and Running QUASES-ARXPS	3
Installing and Running QUASES-IMFP-TPP2M	3
Installing and Running QUASES-SimpleBackgr	4
<b>Chapter 1</b>	
<b>Concept of the QUASES-ARXPS™ analysis procedures</b>	<b>5</b>
<b>Chapter 2</b>	
<b>Principles of QUASES-ARXPS analysis</b>	<b>7</b>
2.1. ARXPS formalism	7
2.2. Depth distribution function (DDF)	8
2.2.1 No elastic electron scattering	8
2.2.2 Elastic electron scattering	8
<b>Chapter 3</b>	
<b>Details of the calculations</b>	<b>11</b>
3.1 Calculation of intensities	11
3.1.1 Intensity from a concentration depth profile	14
3.1.2 Island formation.	16
3.1.3 Final algorithm.	18
3.2 Handling of elastic electron scattering	19
3.3 Normalization	20
3.3.1 Simple Normalization	20
3.3.2 Absolute normalization	21
3.3.3 Relative normalization	23
3.4 Optimization	24
<b>Chapter 4</b>	
<b>User Interface</b>	<b>25</b>
4.1 New Profile Type	26
4.2 Info-frame	28
4.3 Profile-frame	29
4.4 Data-frame	35
4.4.1 Input Data	35

4.4.2 Optimization	38
4.5 Menu Bar	40

## **Chapter 5**

### **File formats 43**

5.1 Save	43
5.2 Open	44

## **Chapter 6**

### **Tutorials 45**

6.1 Simple normalization	45
6.2 Absolute normalization	47
6.3 Relative normalization	49
6.4 Elastic scattering	53

## **References 54**

# Introduction.

Three-dimensional nano-structures are now widely used in technological applications. As a consequence there has been a great demand for analysis techniques that provide quantitative information of surface composition with nano-meter depth resolution and in particular there has been interest in non-destructive techniques.

One such technique developed by Tougaard et al. [1-4] relies on the fact that the energy distribution of emitted electrons depends strongly on the traveled path lengths and thereby also on the in-depth concentration profile. Quantification is then possible by analysis of the peak shape and background of inelastically scattered electrons. A software package for this type of analysis has been available for some time under the name: QUASES-Tougaard™. An alternative technique for non-destructive quantitative surface analysis with nano-meter depth resolution relies on the phenomenon that the angular dependence of the peak intensity varies characteristically with the depth of excitation of the Auger or photon excited electrons. The technique is known as angle-resolved XPS or AES (ARXPS or ARAES). It has been reviewed in several papers [5-12]. The limitations, the problems, and the accuracies that can be achieved with this method were systematically investigated from a theoretical point of view in an excellent paper by Cumpson [12]. He showed that in general the information content is fairly low and that the depth resolution in ARXPS is limited by signal-to-noise ratio as well as systematic errors and not by the number of emission angles for which data is acquired. It is well known that elastic electron scattering has a significant effect on the intensity as a function of emission angle and that this may have a significant influence on the determined overlayer thicknesses. However the applied procedures for ARXPS and ARAES generally neglect this because no simple and practical procedure for correction has been available. Recently, new algorithms have been suggested to correct for elastic scattering effects [13-16]. The efficiency of these algorithms to correct for elastic scattering effects in the interpretation of ARXPS and ARAES was studied in a recent paper [17]. This was done by first calculating electron distributions by Monte Carlo simulations for well-defined overlayer/substrate systems and then to apply the different algorithms. It was found that an analytical formula based on a solution of the Boltzmann transport equation provides a good account for elastic scattering effects [13]. However this procedure is computationally very slow and the underlying algorithm is complicated. Another much simpler algorithm [14], proposed by Nefedov and coworkers, was also tested. Three different ways of handling the scattering parameters within this model were tested and it was found that this algorithm also gives a good description for elastic scattering effects provided that it is slightly modified so that it takes into account the differences in the transport properties of the substrate and the overlayer. In the paper [17], it is found that the heights determined from overlayer/substrate systems determined with this method deviate in general by ~ 10 % or less from the nominal values. The only inputs in the calculations are the inelastic mean free paths and elastic transport mean free paths for the substrate and the overlayer materials.

The QUASES-ARXPS software package takes this correction into account. Besides it provides efficient optimization of parameters to a given set of data.

When, in 2000, we started a systematic study of the validity of ARXPS, we could not find a suitable commercial software package. We felt that to make quantitative surface analysis more widespread and standardized, there is a need for a general tool similar to what has been available for the Tougaard method for some years now in the form of the QUASES™-Tougaard software package. This is the reason why we decided to develop and market a software package to extract depth profile information from ARXPS and ARAES. The QUASES-ARXPS™ software package is the result of this effort. The aim is to provide a practical tool that makes quantification of surface nano-structures by application of ARXPS feasible for routine analysis work.

*January 2002*

*Tommy S. Lassen and Sven Tougaard*

For further information please contact:

Sven Tougaard  
QUASES Tougaard ApS.,  
Ridderhatten 316  
DK-5220 Odense SØ, Denmark.

E-mail: [tougaard@quases.com](mailto:tougaard@quases.com)  
Net: [www.quases.com](http://www.quases.com)

# Installing and Running QUASES-ARXPS™

## System requirements

- A PC with 80486 or higher processor (Pentium 133 MHz or higher is recommended), running Microsoft Win 95, 98, ME, NT, or 2000.
- A CD-ROM disk drive for installation
- A hard disk with 15 MB free disk space
- VGA graphics 600x800 (1024x768 or higher is recommended)
- A mouse

## Installing and Running QUASES-ARXPS™

1. Create a new directory on your hard disk (for example with the name QUASES-ARXPS).
2. Insert the CD in the CD-ROM drive.
3. Open the directory QUASES-ARXPS on the CD.
4. Copy the files “ARXPS.exe” and “TABLE.TXT” and the directory “Test Data” from the CD to the newly created directory on your hard disk.
5. Click ARXPS.exe to start the program.
6. It is recommended to work through the Tutorial examples in Chapter 6.

## Installing and Running QUASES-IMFP-TPP2M™

Note that this program is provided as is without documentation and no service is provided. We hope that you find the program useful for determination of inelastic electron mean free paths.

1. Insert the CD in the CD-ROM drive.
2. Open the directory Install-IMFP-TPP2M on the CD.
3. Click “Setup.exe”

4. Follow the instructions on the screen.
5. To start the program:
  - a. Click the Windows Start button.
  - b. Point to Programs
  - c. Point to QUASES-Tougaard
  - d. Click the IMFP-TPP2M icon.

## **Installing and Running QUASES-SimpleBackgr™**

Note that this program is provided as is without documentation and no service is provided. We hope that you find the program useful for determination of peak areas.

1. Insert the CD in the CD-ROM drive.
2. Open the directory Install-QUASES-SimpleBackgr on the CD.
3. Click “Setup.exe”
4. Follow the instructions on the screen.
5. To start the program:
  - a. Click the Windows Start button.
  - b. Point to Programs
  - c. Point to QUASES-Tougaard
  - d. Click the QUASES-Simple\_Backgrounds icon.

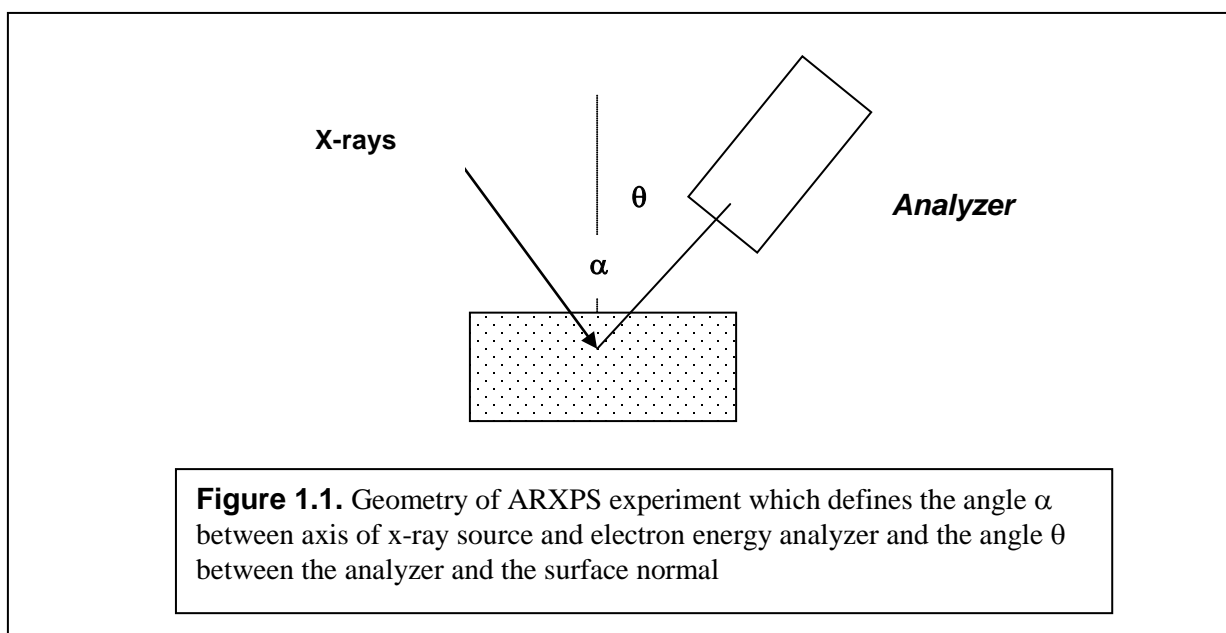
# Chapter 1

## Concept of the QUASES-ARXPS™ analysis procedures

Chapters 1 and 2 describe the principle of analysis used in QUASES-ARXPS. If you are already familiar with these ideas you can skip this chapter and continue in Chapter 3.

In a photoelectron spectrum, the intensity of excited core electrons into the solid angle  $\Omega$ ,  $d\Omega$  is given by the cross section

$$\frac{d\sigma_{nl}(\Omega, E)}{d\Omega} = \frac{\sigma_{nl}(E)}{dE} \frac{1}{4\pi} \left[ 1 - \frac{\beta_{nl}}{4} (3\cos\alpha - 1) \right] \quad (1.1)$$



where  $d\sigma_{nl}$  is the photoelectron cross section and  $\beta_{nl}$  is the asymmetry parameter.  $\alpha$  is the angle between the x-ray source and the analyzer axis, see figure 1.1. Quantitative surface chemical composition analysis by X-ray photoelectron or Auger electron spectroscopy (XPS or AES) relies on several factors like for example knowledge of photoionization cross sections, inelastic electron mean free paths, and the influence of elastic electron scattering. The most serious problem in quantitative XPS, that gives the largest contribution to errors of analysis, is however assumptions made on the in-depth distribution of atoms. To be able to extract quantitative information from a measured peak intensity, it is necessary to make an assumption, and for convenience it is usually assumed that the surface region is homogeneous up to a depth of a few nano-meters. This assumption does however make quantification of surface chemical compositions by XPS and AES extremely unreliable as shown below.

In the majority of routine quantitative applications of surface sensitive electron spectroscopies, the user is primarily interested in the composition of the solid within the sampling depth of these techniques. However, in most cases, the composition varies with depth, and the quantitative analysis provides then an averaged composition. Much work has been done in the past to develop analytical procedures that provide quantitative information on the actual in-depth concentration profile from analysis of AES or XPS. One such technique developed by Tougaard et al. [1-4] relies on the fact that the energy distribution of emitted electrons depends strongly on the traveled path lengths and thereby also on the in-depth concentration profile. Another technique [5-12] relies on the phenomenon that the angular dependence of the peak intensity varies characteristically with the depth of excitation of the Auger or photon excited electrons. The latter technique is the subject of the QUASES-ARXPS software package. The acronyms of ARXPS and ARAES (angle-resolved XPS or AES) have been coined for these procedures. In an excellent paper by Cumpson [12], the limitations, the problems, and the accuracies that can be achieved with this method were systematically investigated from a theoretical point of view. Similar extensive experimental investigations have not been done.

The effects of elastic electron scattering in electron spectroscopies were summarized in an extensive review [13]. The early reports on the influence of elastic collision on the ARXPS results referred to overlayer thickness measurements performed at different emission angles. Baschenko and Nefedov [7] have indicated that the drastically small values of the overlayer thickness determined from XPS intensities by Ebel [8] at glancing emission angles may be ascribed to the neglect of elastic photoelectron scattering in the applied formalism. In a later report, Ebel *et al.* [9] proved that the influence of elastic scattering on the measured overlayer thicknesses is more complex. For small emission angles, the calculated overlayer thickness is overestimated due to the neglect of elastic scattering while for large emission angles it tends to be underestimated. In this range of angles, the finite solid acceptance angle of the analyzer may further increase these effects.

## Chapter 2

# Principles of QUASES-ARXPS™ analysis

### 2.1. ARXPS formalism

The ARXPS formalism is founded on a simple expression that relates the measured photoelectron intensity,  $I^{nel}$ , with the concentration profile,  $c(z)$

$$I^{nel} = I_0 \int_0^{\infty} c(z) \phi^{nel}(z, \theta) dz = I_0 \int_0^{\infty} c(z) \exp\left(-\frac{z}{\lambda_i \cos \theta}\right) dz \quad (2.1)$$

where  $\lambda_i$  is the inelastic electron mean free path,  $\theta$  the angle of emission with respect to the surface normal and  $I_0 \lambda_i \cos \theta$  is the intensity recorded from a solid with  $c(z) \equiv 1$ . The index *nel* indicates that elastic photoelectron collisions have been neglected in eq.(1). To calculate the intensity  $I^{el}$  with account for elastic photoelectron collisions, we need to know the actual depth distribution function,  $\phi^{el}(z, \theta)$  [13]

$$I^{el} = I_0 \int_0^{\infty} c(z) \phi^{el}(z, \alpha) dz \quad (2.2)$$

Jablonski and Tougaard [16] introduced the correcting function  $CF$  into the ARXPS formalism

$$I^{el} = I_0 \int_0^{\infty} CF(z, \alpha) c(z) \exp\left(-\frac{z}{\lambda_i \cos \alpha}\right) dz \quad (2.3)$$

where

$$CF(z, \alpha) = \frac{\phi^{el}(z, \alpha)}{\phi^{nel}(z, \alpha)} \quad (2.4)$$

In this way, the problems with normalizing the DDF were avoided.

Elastic electron scattering effects may be taken into account by Monte Carlo simulations of electron transport. Such calculations are however extremely time consuming and this is not relevant for practical ARXPS analysis. It is therefore of interest first of all to know to what extent the calculated depth profile is affected by the neglect of elastic scattering effects in the ARXPS formalism.

Secondly, it is of interest to find analytical formulas that are sufficiently fast that they may be applied in practical ARXPS data analysis and still give a reasonably accurate description. To approach this problem, we need an analytical expression for the DDF function which has been obtained from a realistic theory that accounts for elastic photoelectron collisions. Several such expressions are available in the literature [16, 18-24]. They were derived from two procedures:

1. Analytical expressions derived from electron transport theory [16, 23-24]
2. Fit of an analytical expression to the results of Monte Carlo calculations [18-22].

The validity of these procedures were compared in a recent publication [17].

## 2.2. Depth distribution function (DDF)

### 2.2.1 No elastic electron scattering

In the straight line approximation where elastic electron deflection is ignored the DDF is

$$\phi = \exp\left(-\frac{z}{\lambda_i \cos\theta}\right) \quad (2.5)$$

### 2.2.2 Elastic electron scattering

In general the correction procedures for elastic electron scattering are complex because it varies with the geometry of the experiment and the details of the sample composition. In many cases an approximate account for elastic scattering effects can be obtained by using attenuation lengths instead of IMFPs in the simple expression eq.(2.1) (see e.g. Cumpson and Seah [25]). A more general procedure which leads to a relatively simple analytical expression for the DDF has been derived by Nefedov and Fedorova [23] and Nefedov [14]

$$\phi^{el}(z, \theta) = \phi_i(z, \theta, \omega) + \frac{\beta}{4} \phi_a(z, \theta, \omega) \quad (2.6)$$

where the index  $i$  denotes the isotropic contribution to the DDF, and the index  $a$  the anisotropic contribution. The parameter  $\omega$  is the single scattering albedo

$$\omega = \frac{\lambda_i}{\lambda_i + \lambda_{tr}} \quad (2.7)$$

where  $\lambda_{tr}$  is the transport mean free path for elastic electron scattering. Eq(2.6) is a semi-empirical formula derived from electron transport theory and by fitting to Monte-Carlo simulations.

The following expression has been found to compare well with Monte Carlo simulations for emission angles up to  $\sim 60 - 75^\circ$  and for depths  $z$  up to  $5 \lambda_i$  [14, 23].

$$\phi_i^{\text{mod}}(z, \theta, \omega) = \phi_i(z, \theta, \omega) \exp(-z / \lambda_i) + \phi_i(z, \theta, 1.3\omega) [1 - \exp(-z / \lambda_i)] \quad (2.8)$$

$$\phi_i(z, \omega) = H(\mu, \omega) \left[ 0.5 \exp(-z / c \lambda_i \mu) + 0.5 \frac{(\nu_0 c - \mu) \exp(-z / c^2 \mu \lambda_i) + \mu(1 - c) \exp(-z / c^2 \lambda_i \nu_0)}{c(\nu_0 - \mu)} \right] \quad (2.9)$$

where  $c = (1 - \omega)^{0.5}$ ,  $\mu = \cos \theta$ ,  $H(\mu, \omega)$  is the Chandrasekhar function, and  $\nu_0$  is the root of the equation

$$1 = \frac{\omega \nu_0}{2} \ln \frac{\nu_0 + 1}{\nu_0 - 1} \quad (2.10)$$

For small values of  $\omega$ , Eq. (2.10) simplifies to

$$\nu_0 = 1 + 2 \exp(-2 / \omega) \quad (2.11)$$

The anisotropic contribution to the DDF is given by

$$\phi_a(z, \theta, \omega) = \exp(-z / c^2 \lambda_i \mu) (3 \cos^2 \alpha - 1) \quad (2.12)$$

where  $\alpha$  is the angle between the direction of x-rays and the direction of photoelectron emission from the surface.

The above results are based on the transport approximation in which the angular dependence of the elastic scattering cross section is described by a single parameter i.e. the transport mean free path. It is obvious that more accurate DDFs are expected to be obtained from Monte Carlo simulations of the photoelectron transport in the solid since this approach uses the actual angular structure of the differential elastic scattering cross sections.

As mentioned above, Monte Carlo simulations usually require a considerable computational effort and for this reason they are not relevant for practical quantitative analysis. The validity of these procedures to correct for elastic electron scattering effects in ARXPS were compared in a recent publication [17], where extensive Monte Carlo generated data were corrected by the various methods.

It was found that the simple analytical formula given by eqs.(2.6) gives a good description provided that it is slightly modified so that it takes into account the differences in the transport properties of the substrate and the overlayer. It is found that the heights determined from overlayer/substrate systems determined with this method deviate in general by  $\sim 10\%$  or less from the nominal values. The only inputs in the calculations are the inelastic mean free paths and elastic transport mean free paths for the substrate and the overlayer materials. Since it is simple and yet of reasonable accuracy, this is the procedure that is implemented in the QUASES-ARXPS software package.

# Chapter 3

## Details of the calculations

### 3.1 Calculation of intensities

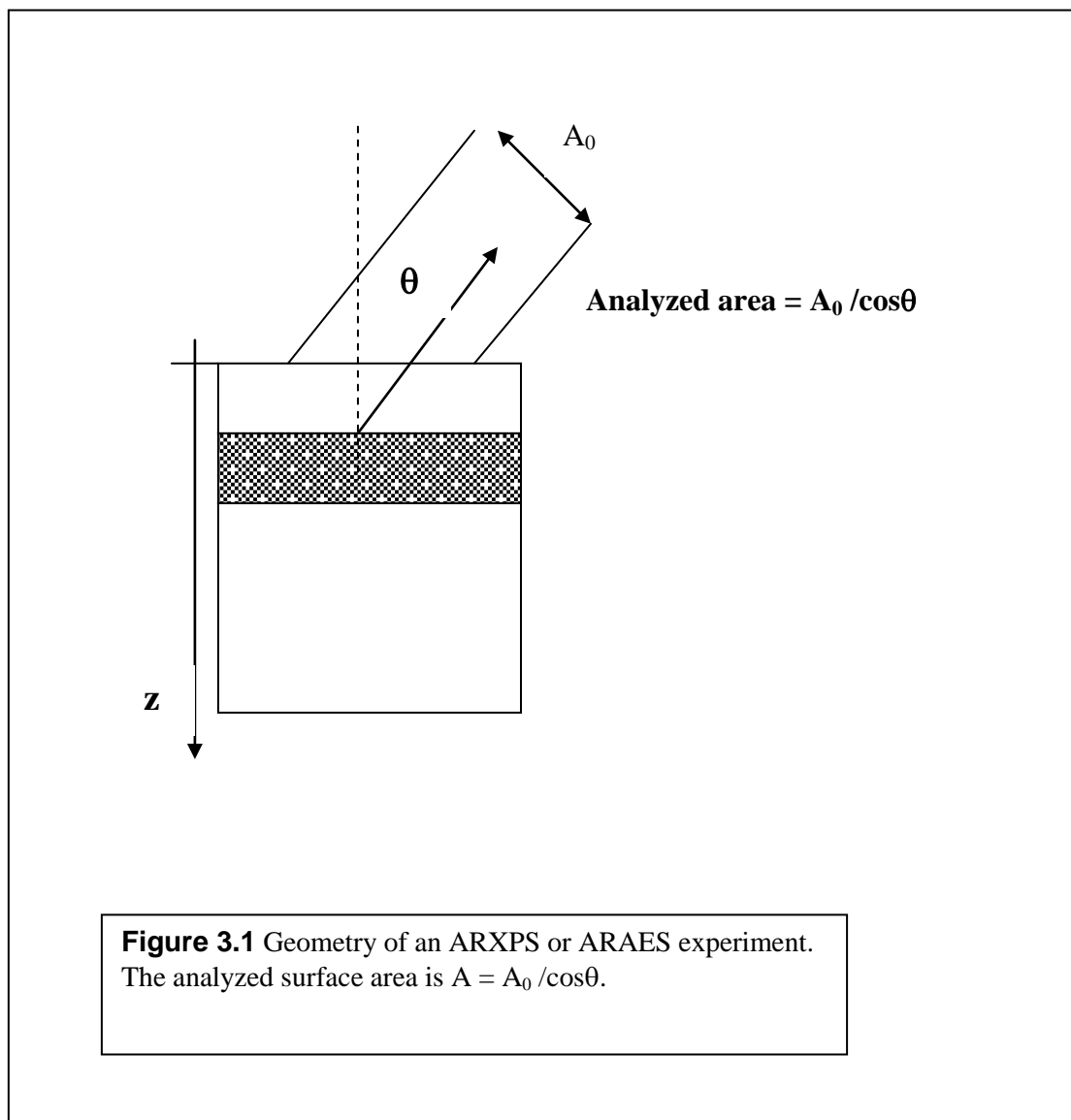


Fig. 3.1 shows the geometry of the ARXPS or ARAES experiment. Assuming that atoms at depth  $z$  with density  $c(z)$  emits Auger or Photo- electrons and that the electron energy analyzer is at an angle  $\theta$  to the surface normal. Then the contribution to the intensity collected by the analyzer from electrons excited at the layer  $dz$  at depth  $z$  is

$$dI(\theta) = \frac{A_0}{\cos\theta} \phi(z, \theta) \cdot c(z) \cdot dz \quad (3.1)$$

where  $\phi(z, \theta)$  is the probability that an electron excited at depth  $z$  escapes the solid surface without energy loss. This is the Depth Distribution Function (DDF).

When elastic scattering is neglected,

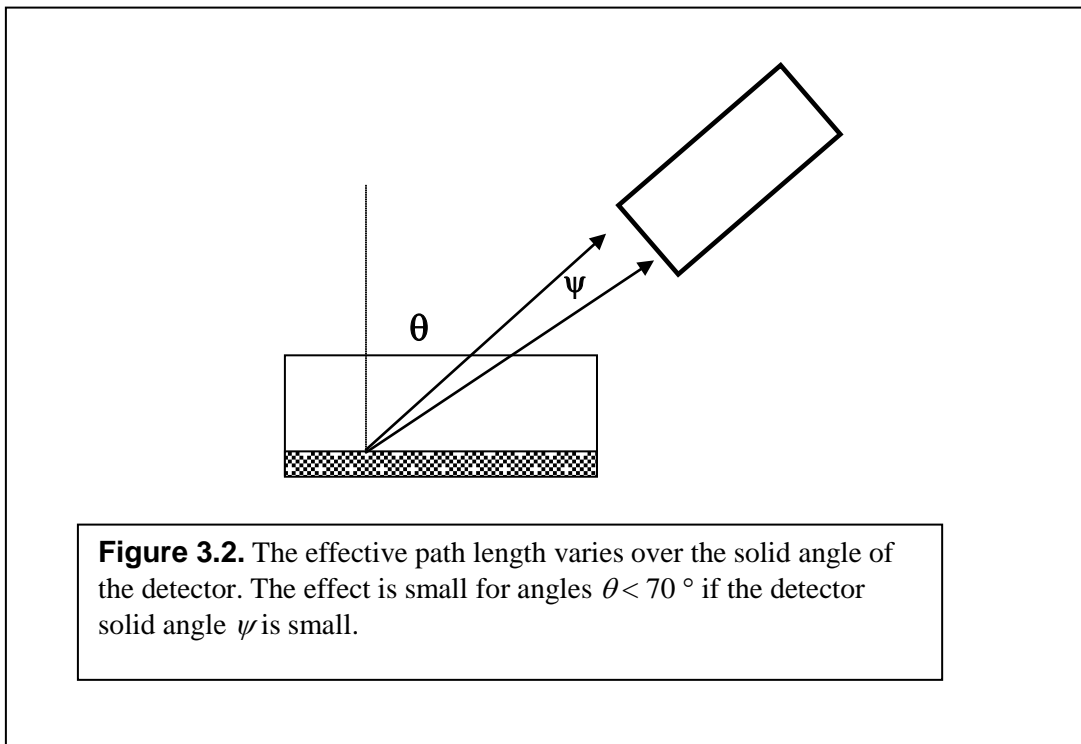
$$\phi(z, \theta) = \exp(-z / \lambda \cdot \cos\theta) \quad (3.2)$$

The intensity may be written

$$I(\theta) = \frac{A_0}{\cos\theta} \cdot (DF) \cdot (XF) \cdot \int_0^{\infty} c(z_{eff}) \cdot \phi(z_{eff}, \theta) \cdot dz \quad (3.3)$$

where

- $DF$  describes the detector efficiency and
- $XF$  describes excitation probability and contains specifications of the the x-ray flux density and the photo- or Auger- electron excitation cross section.



The DDF  $\phi(z_{eff}, \theta)$  depends on an effective path length  $z_{eff}$  for the electrons that enter the detector. This is an effect due to the finite analyzer acceptance angle which cause the path lengths to vary for electrons that enter various parts of the detector solid angle (see figure 3.2). The effective pathlength can be expressed  $z_{eff} = (1 + f(\psi, \theta)) \cdot z$  where  $\psi$  is the solid angle of the analyzer [26]. The effect is usually small ( $f(\psi, \theta) < 0.1$  for  $0^\circ < \theta < 70^\circ$  when  $\psi < 9^\circ$ ) and it is not included in the present software. Then

$$I(\theta) = \frac{A_0}{\cos\theta} \cdot (DF) \cdot (XF) \cdot \int_0^\infty c(z) \cdot \phi(z, \theta) \cdot dz \quad (3.4)$$

### 3.1.1 Intensity from a concentration depth profile.

To calculate the intensity from a given concentration depth profile, the structure is divided into layers as illustrated in figure 3.3.

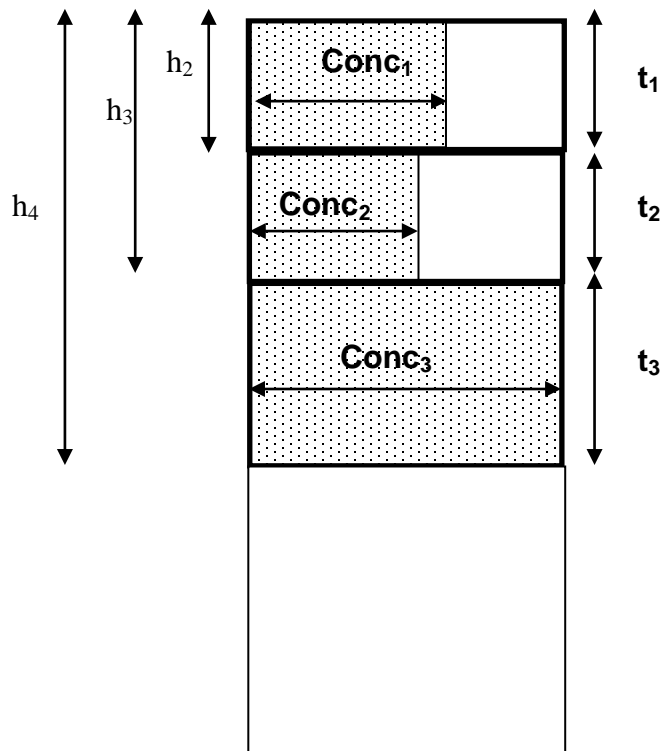


**Figure 3.3.** Example of a solid consisting of three layers of thickness  $t_1$ ,  $t_2$  and  $t_3$  on a passive substrate. All three layers 1, 2 and 3 cover 100 % of the surface but the atomic concentration is different. The concentration in layers 1, 2 and 3 are 60 %, 50 % and 100 %

In the straight line approximation, the attenuation of electron intensity that pass through layer  $X$ , which extends from depth  $h_X$  to  $h_X + t_X$  is

$$D_X = \exp(-t_X / \lambda_X \cos \theta) \quad (3.5)$$

When elastic scattering is included an approximate expression is

$$D_X = \frac{\phi_X(t_X + h_X, \theta)}{\phi_X(h_X, \theta)} \quad (3.6)$$

The emitted intensity from a layer  $n$  that extends from  $h_n$  to  $h_n + t_n$  is then

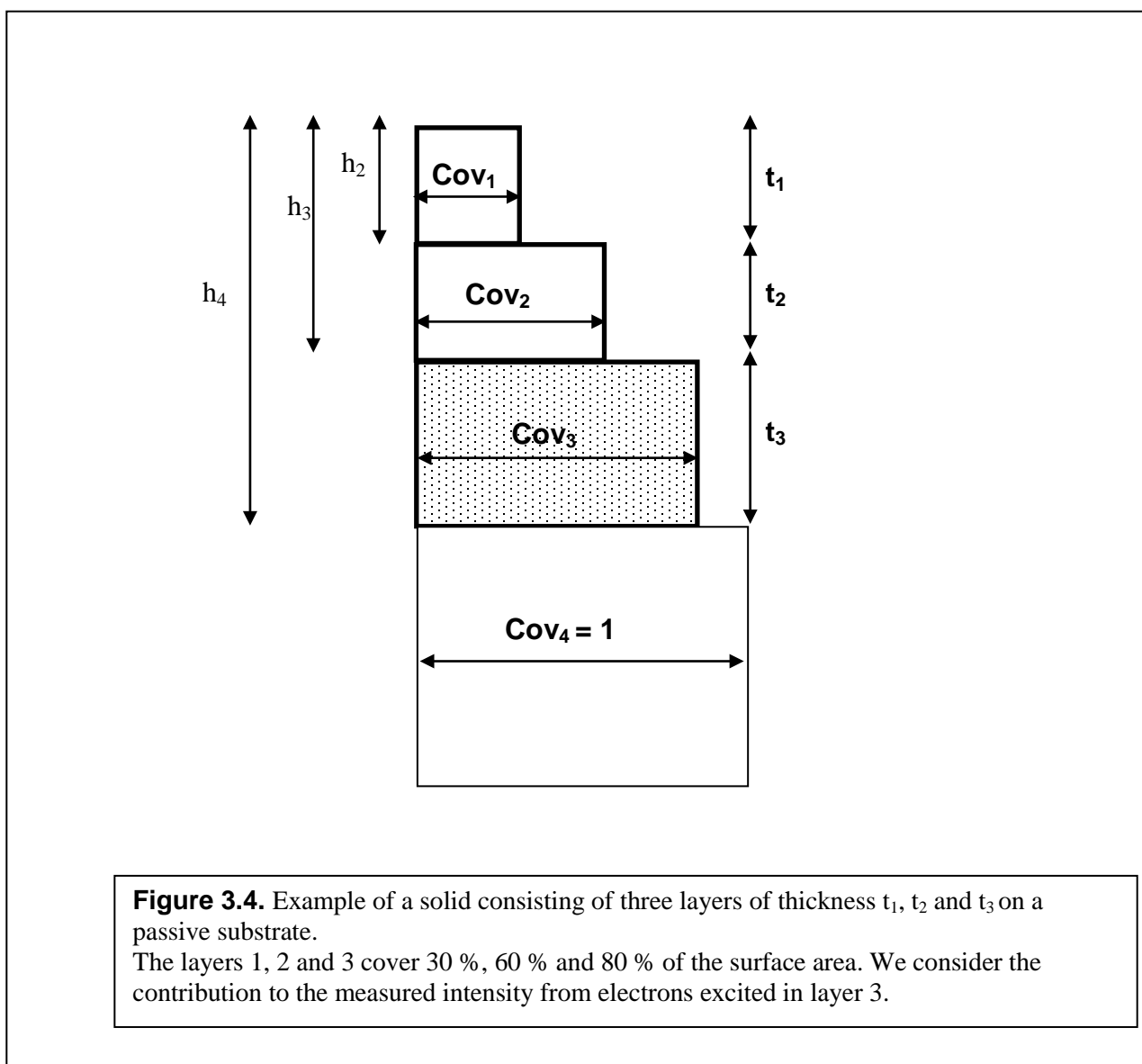
$$I_n = \left( \int_0^{t_n} \text{conc}_n \cdot \phi_n(z, \theta) \cdot dz \right) \cdot \prod_{X=1}^{n-1} D_X \quad (3.7)$$

and the total emitted intensity from the layered structure in figure 3.3 is

$$I = \sum_{n=1}^N I_n \quad (3.8)$$

### 3.1.2 Island formation.

To handle the situation where islands of varying thickness and concentration are formed on the surface, the following description is used to calculate the measured intensity distributions that can be compared with measured intensities. The intensity from a given layer is divided into fractions of electrons that have passed the layers above the layer where the electrons are created. This division is only strictly possible in the Straight line approximation where elastic scattering is neglected.



To illustrate the principle, the intensity from layer 3 in figure 3.4 is

$$I_3 = I_{3,1} + I_{3,2} + I_{3,3} \quad (3.9)$$

where

$$I_{3,1} = Cov_1 \cdot \left( \int_0^{t_3} conc_3 \cdot \phi_3(z) \cdot dz \right) \cdot D_2 \cdot D_1$$

$$I_{3,2} = (Cov_2 - Cov_1) \cdot \left( \int_0^{t_3} conc_3 \cdot \phi_3(z) \cdot dz \right) \cdot D_2$$

$$I_{3,3} = (Cov_3 - Cov_2) \cdot \left( \int_0^{t_3} conc_3 \cdot \phi_3(z) \cdot dz \right)$$

### 3.1.3 Final algorithm.

The final algorithm in the program combines the effects in the above two sections. I.e. for each layer both the concentration and the coverage may vary. The parameters to describe the structure is shown in figure 3.5. In the program, the user inputs for each layer values for  $Cov$ ,  $Conc$ ,  $t$ , and the inelastic mean free path  $\lambda_i$ .

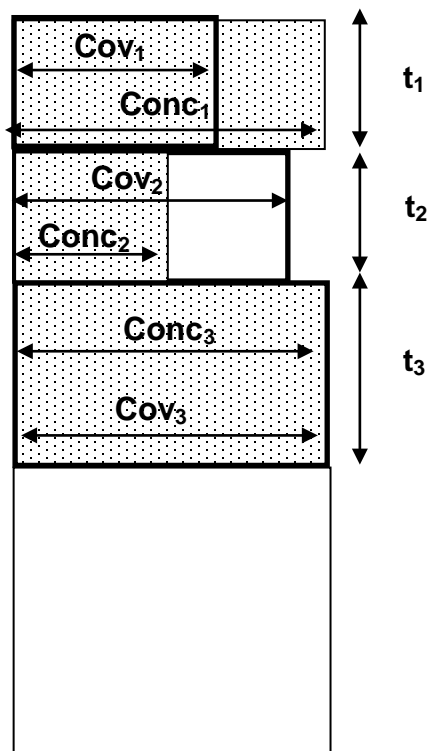


**Figure 3.5.** Example of solid consisting of three layers of thickness  $t_1$ ,  $t_2$  and  $t_3$  on a passive substrate. The coverage of layers 1, 2 and 3 are 60 %, 90 %, and 100 %, and the concentration in layers 1, 2 and 3 are 100 %, 50 % and 100 %

### 3.2 Handling of elastic electron scattering

Elastic electron scattering is described by the approximate formula for the DDF by Nefedov [14] as outlined in Chapter 2. The elastic scattering effects are described by the transport mean free path for elastic electron scattering  $\lambda_{tr}$ . The elastic scattering effects varies with the angular distribution of excited electrons. For XPS this is given by the asymmetry parameters  $\beta$  and the angle  $\alpha$  between incoming x-rays and the analyzer axis and these two parameters must be input when elastic scattering correction is included.

Eq.3.7 is exact when inelastic scattering for the layers are different as long as elastic scattering is neglected.

Elastic scattering is described by eq.(2.2). The algorithm eq.(2.6) of Nefedov for  $\phi^{el}$  is strictly valid only when both elastic and inelastic scattering properties of all layers are identical.

When this is not the case, eq.(3.7) may be applied as an approximation. This is used in the *QUASES-ARXPS* program when different values  $\lambda_i$  and  $\lambda_{tr}$  are applied for each layer. When they vary considerably for the different layers, the accuracy of the elastic scattering correction is diminished.

### 3.3 Normalization

Intensities are hardly ever measured on an absolute scale and therefore intensities must be normalized before comparison with theory is possible. There are different ways this can be done.

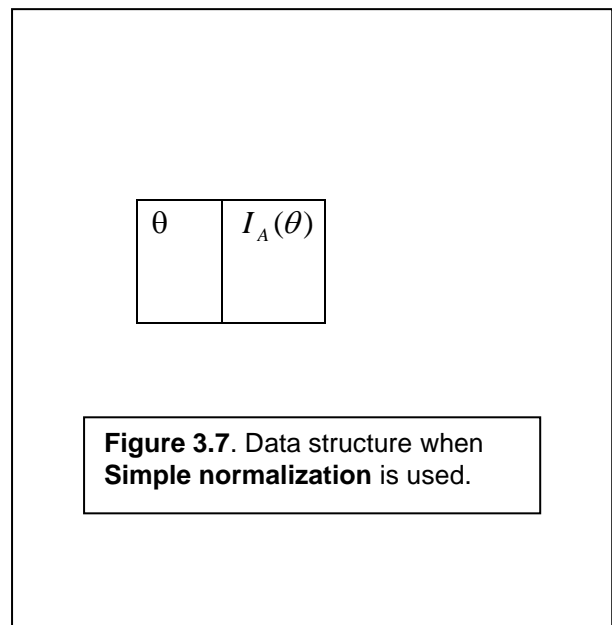
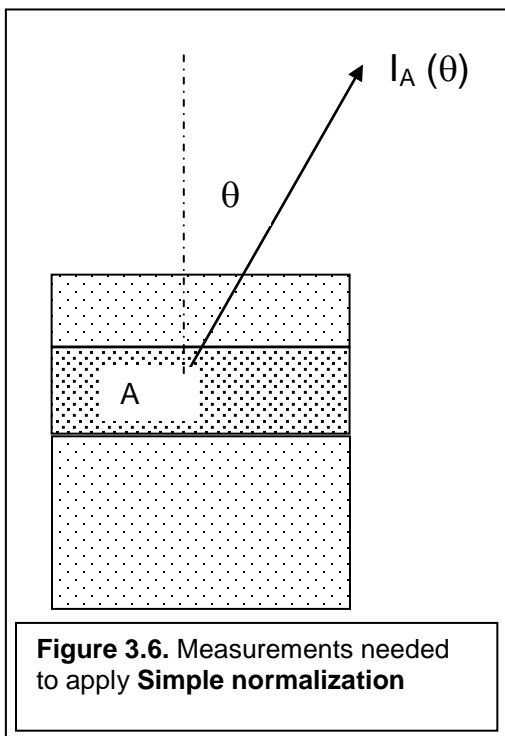
#### 3.3.1 Simple Normalization

Here the normalization is done relative to an angle from the set of intensities from a single peak. For a data set  $I_A(\theta)$  this is done by normalizing to the intensity at one of the measured angles  $\theta_{num}$ . If the variation of  $DX$  and  $XF$  with  $\theta$  can be neglected we get from Eq.(3.4)

$$\left[ \frac{I_A(\theta)}{I_A(\theta_{num})} \right]_{\text{experiment}} = \frac{\cos \theta_{num}}{\cos \theta} \cdot \frac{\int_0^\infty c_A(z) \cdot \varphi(z, \theta) \cdot dz}{\int_0^\infty c_A(z) \cdot \varphi(z, \theta_{num}) \cdot dz} \quad (3.11)$$

and from this it follows that

$$\frac{\int_0^\infty c_A(z) \cdot \varphi(z, \theta) \cdot dz}{\int_0^\infty c_A(z) \cdot \varphi(z, \theta_{num}) \cdot dz} = \frac{\cos \theta}{\cos \theta_{num}} \cdot \left[ \frac{I_A(\theta)}{I_A(\theta_{num})} \right]_{\text{experiment}} \quad (3.11a)$$



The experimental points are plotted as

$$\frac{\cos \theta}{\cos \theta_{num}} \cdot \left[ \frac{I_A(\theta)}{I_A(\theta_{num})} \right]_{\text{experiment}} \quad (3.12a)$$

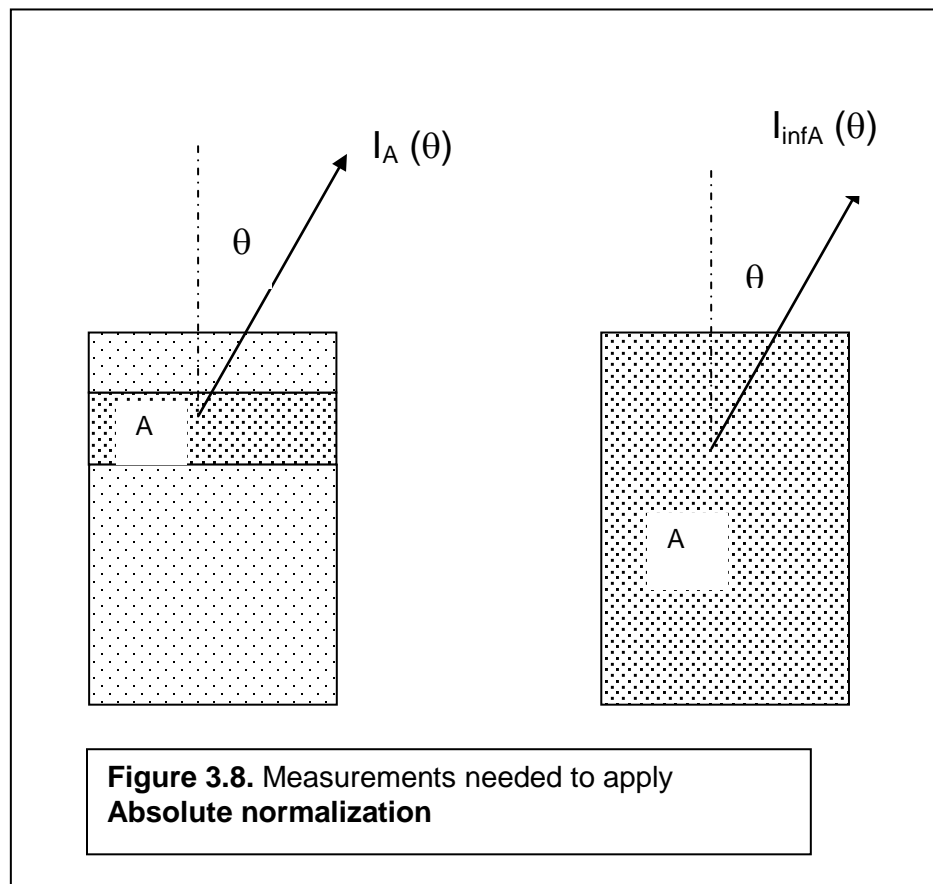
The QUASES-ARXPS program calculates and plots the theoretical values

$$\left[ \frac{I_A(\theta)}{I_A(\theta_{num})} \right]_{\text{theory}} = \frac{\int_0^{\infty} c_A(z) \cdot \varphi(z, \theta) \cdot dz}{\int_0^{\infty} c_A(z) \cdot \varphi(z, \theta_{num}) \cdot dz} \quad (3.12b)$$

Input in the program must be a list of values of  $\theta$  and  $I_A(\theta)$  as in figure 3.7.

### 3.3.2 Absolute normalization

Here intensities are normalized to the intensities from a reference sample of a pure infinite solid of the same atoms and at the same angles of emission (see figure 3.8). Denoting this intensity  $I_{inf A}(\theta)$  we get



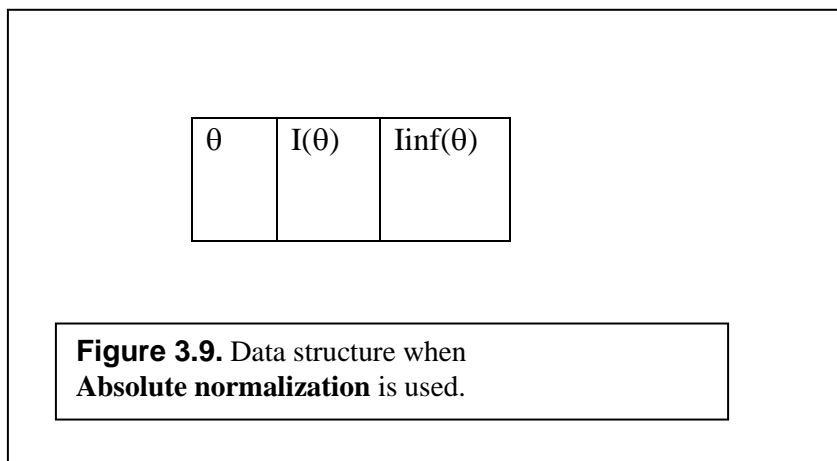
$$\left[ \frac{I_{\text{inf}A}(\theta)}{I_{\text{inf}A}(\theta_{\text{num}})} \right]_{\text{theory}} = \frac{\int_0^\infty c_{\text{inf}A} \cdot \varphi(z, \theta) \cdot dz}{\int_0^\infty c_{\text{inf}A} \cdot \varphi(z, \theta_{\text{num}}) \cdot dz} = \frac{\int_0^\infty \varphi(z, \theta) \cdot dz}{\int_0^\infty \varphi(z, \theta_{\text{num}}) \cdot dz} \quad (3.13)$$

The QUASES-ARXPS program calculates

$$\frac{I_A(\theta) \cdot \int_0^\infty \varphi(z, \theta_{\text{num}}) \cdot dz}{I_A(\theta_{\text{num}}) \cdot \int_0^\infty \varphi(z, \theta) \cdot dz} = \frac{\int_0^\infty c_A(z) \cdot \varphi(z, \theta) \cdot dz}{\int_0^\infty c_A(z) \cdot \varphi(z, \theta_{\text{num}}) \cdot dz} \cdot \frac{\int_0^\infty \varphi(z, \theta_{\text{num}}) \cdot dz}{\int_0^\infty \varphi(z, \theta) \cdot dz} \quad (3.14)$$

Input in the program must be a list of values as in figure 3.9.

Note that the dependence on  $c_A(z)$  is weak and the analysis is rather independent of the concentration. When **Absolute normalization** is used, the concentration can therefore usually not be determined with any useful degree of accuracy



### 3.3.3 Relative normalization

Here intensities of one peak from atoms of type “A” are normalized to the intensities of a peak from atoms of type “B” in the same solid. Denoting these intensities  $I_A(\theta)$ , and  $I_B(\theta)$  the QUASES-ARXPS program compares

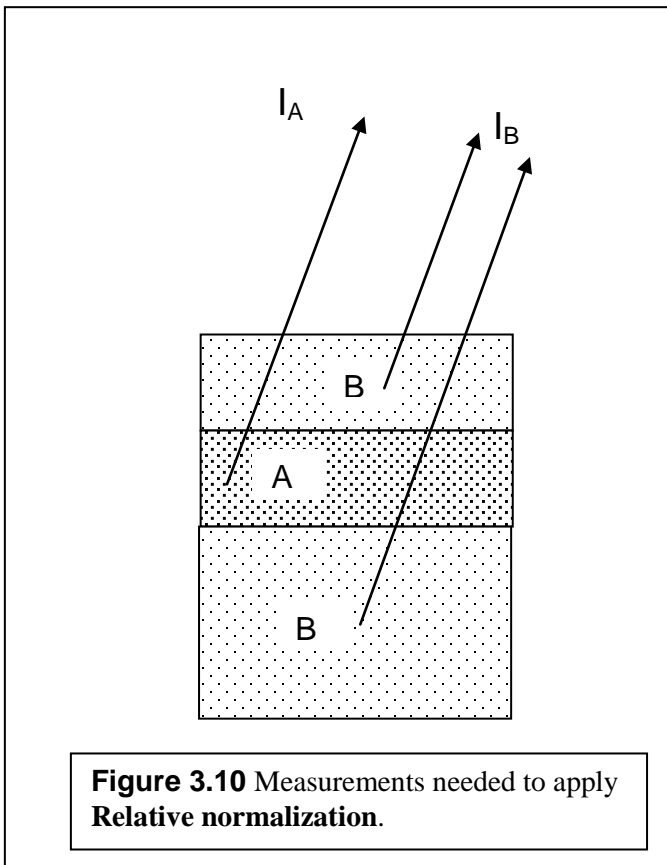
$$\left[ \frac{I_A(\theta)}{I_B(\theta)} \right]_{\text{experiment}} \quad (3.15)$$

to the theoretical value

$$\left[ \frac{I_A(\theta)}{I_B(\theta)} \right]_{\text{theory}} = \frac{\int_0^{\infty} c_A(z) \cdot \varphi_A(z, \theta) \cdot dz}{\int_0^{\infty} c_B(z) \cdot \varphi_B(z, \theta) \cdot dz} \quad (3.16)$$

Input in the program must be a list of values as in figure 3.11

Note that the expression depends strongly on both  $c_A(z)$  and  $c_B(z)$ . Relative normalization gives therefore considerable information on both  $c_A(z)$  and  $c_B(z)$ .



$\theta$	$I_A(\theta)$	$I_B(\theta)$

**Figure 3.11** Data structure when Relative normalization is used.

### 3.4 Optimization

The *RMS* deviation is used to evaluate the quality of the agreement between the model and the experiment. We denote the ratios

$$R_{theory,k} = \left[ \frac{I_A(\theta_k)}{I_B(\theta_k)} \right]_{theory} \quad (3.17)$$

$$R_{exp,k} = \left[ \frac{I_A(\theta_k)}{I_B(\theta_k)} \right]_{experiment} \quad (3.18)$$

where  $R_{theory,k}$  is the calculated ratio corresponding to the assumed surface structure and for the  $k$ th emission angle, and  $R_{exp,k}$  is the measured ratio of intensities for the same emission angle.

The following formula for the RMS gives equal weight to the intensities at all measured emission angles.

$$RMS = \sqrt{\frac{1}{N} \sum_{k=1}^N \left\{ \frac{R_{theory,k} - R_{exp,k}}{R_{theory,k}} \right\}^2} \quad (3.19)$$

where  $N$  is the number of considered emission angles,

It is however often an advantage to give less weight to emission angles with small intensities since these will be most influenced by both systematic errors as well as signal noise. The following RMS value gives less weight to the small intensity ratios.

$$RMS = \sqrt{\frac{1}{N} \sum_{k=1}^N \{R_{theory,k} - R_{exp,k}\}^2} \quad (3.20)$$

Optimization can be done in the program with respect to either eq. (3.19) or eq. (3.20).

# Chapter 4

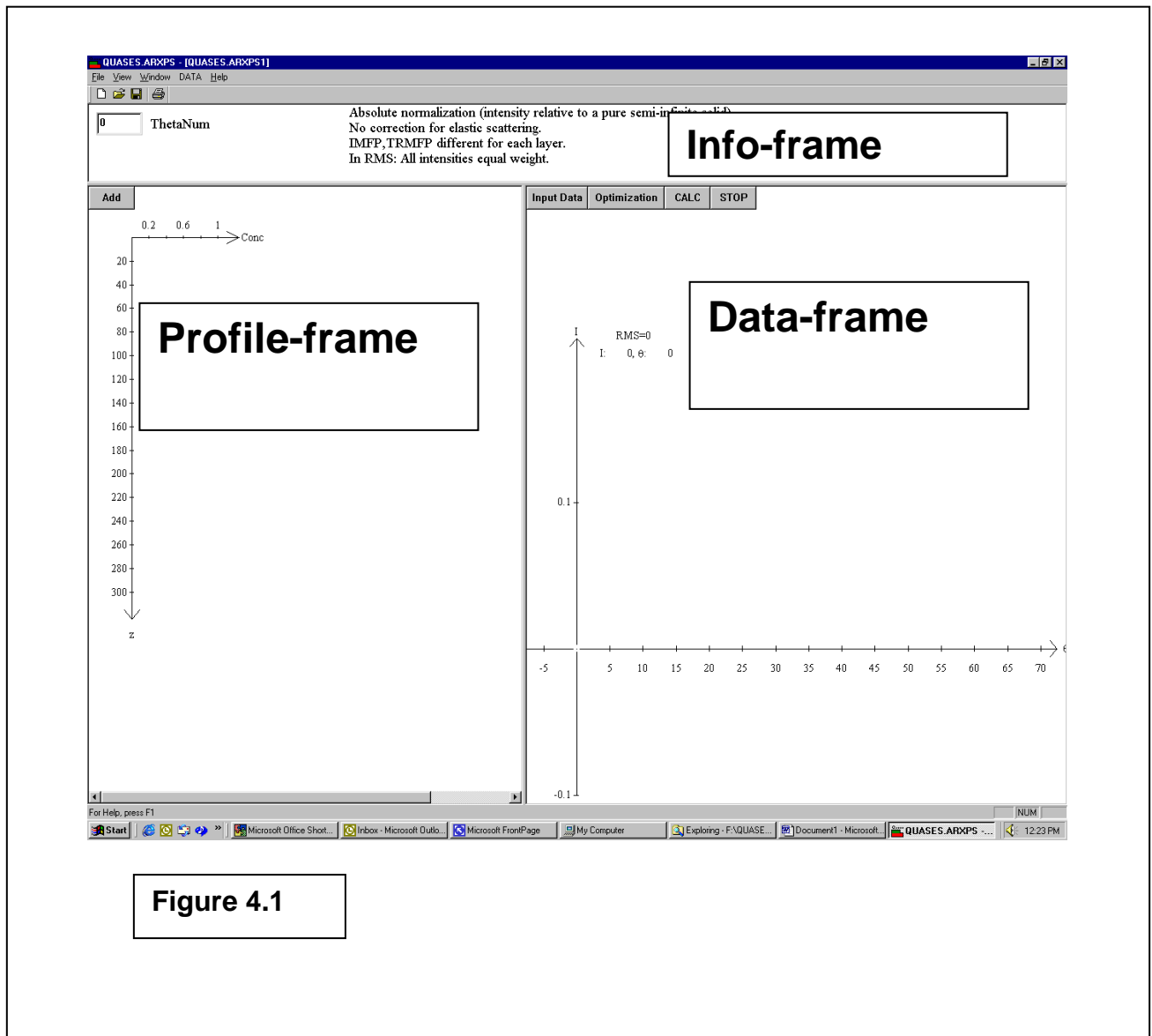
## User Interface

Fig 4.1 shows the user interface after starting the program.  
The interface consists of three frames

- Info-frame
- Profile-frame
- Data-frame

and a

- menu bar.



## 4.1 New Profile Type

To set up a calculation scheme, click the menu bar item **DATA** and then click **New Profile Type** to get fig. 4.2 with a new dialog box with four items.

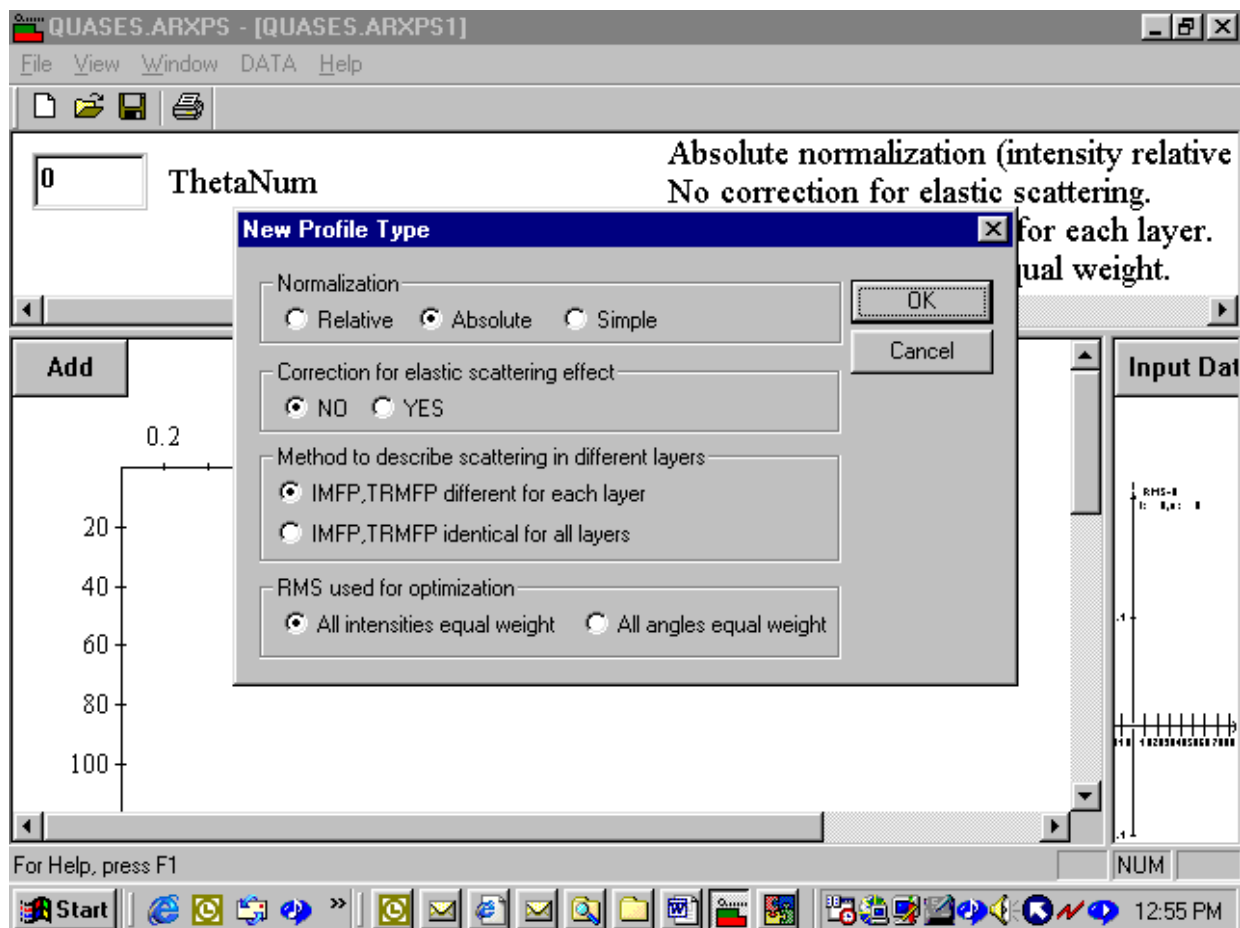


Figure 4.2

In the first item **Normalization**, the user selects the type of data normalization to be used (see Section.3.3).

In the second item **Correction for Elastic Scattering Effect**, the user specifies if elastic scattering effects should be ignored or calculated as described in Sections 3.2 and Chapter 2.

In the third item **Method to describe scattering in different layers**, the user can specify whether or not the calculations should be done under the assumption that

the IMFP and TRMFP are identical for each layer. The calculations are done as described in Secs. 3.1 and 3.2 and as summarized in Table 4.1

Elastic scattering	IMFP, TRMFP	
	Identical	Different
<b>No</b>	Eq.(3.7) with eq.(2.5); exact.	Eq.(3.7) with eq.(2.5); exact.
<b>Yes</b>	Eq.(2.2) with eq.(2.6); "exact".	Eq.(3.7) with eq.(2.6); approximate

**Table 4.1**

In the fourth item **RMS used for optimization** the user can specify whether eq. 3.19 (all angles equal weight) or eq. 3.20 (all intensities equal weight) should be used for optimization of the structure (see Section 3.4)

## 4.2 Info-frame

In the center part of the **Info-frame** (Fig. 4.1), the setup options chosen in **New Profile Type** are summarized.

If **Absolute** or **Simple Normalization** was chosen, a textbox **ThetaNum** is shown (see figure 4.1). This is the angle  $\theta_{num}$  used for normalization of the data as in eqs.(3.11)- (3.14). To set a new value, click the text box and type the value. The program will use the angle in the experimental data-set which is closest to the value set in the text box.

If **Correction for elastic scattering effect** was set to **Yes** in **New Profile Type**, two text boxes with parameters for  $\alpha$  and  $\beta$  appear.  $\alpha$  is the angle between the x-rays and the analyzer (see figure 1.1) and  $\beta$  is the asymmetry-parameter for the photo-excitation. If **Relative Normalization** is used (see eq.(3.16)), values of  $\beta$  for “A” and “B” type atoms are required. Note that for chemically shifted peaks as in the case of Si2p or Si2s in Si/SiO<sub>2</sub>-systems,  $\beta$  is the same for both peaks. Values for  $\beta$  may be found in [27]. To set the parameter values, click the text boxes and type the value.

When the **Optimization** option in the **Data-frame** (see below) is chosen, the number of iterations at any given time is shown in the center and the 4 best RMS values found so far is shown in the far right part of the **Info-frame**.

### 4.3 Profile-frame

In the **Profile-frame** the assumed concentration profile and the scattering properties of the individual layers is specified.

To get figure 4.3, right click the **ADD** button which inserts a layer in the profile.,  
To activate the layer, place the mouse cursor over the layer and right click. The layer turns red.

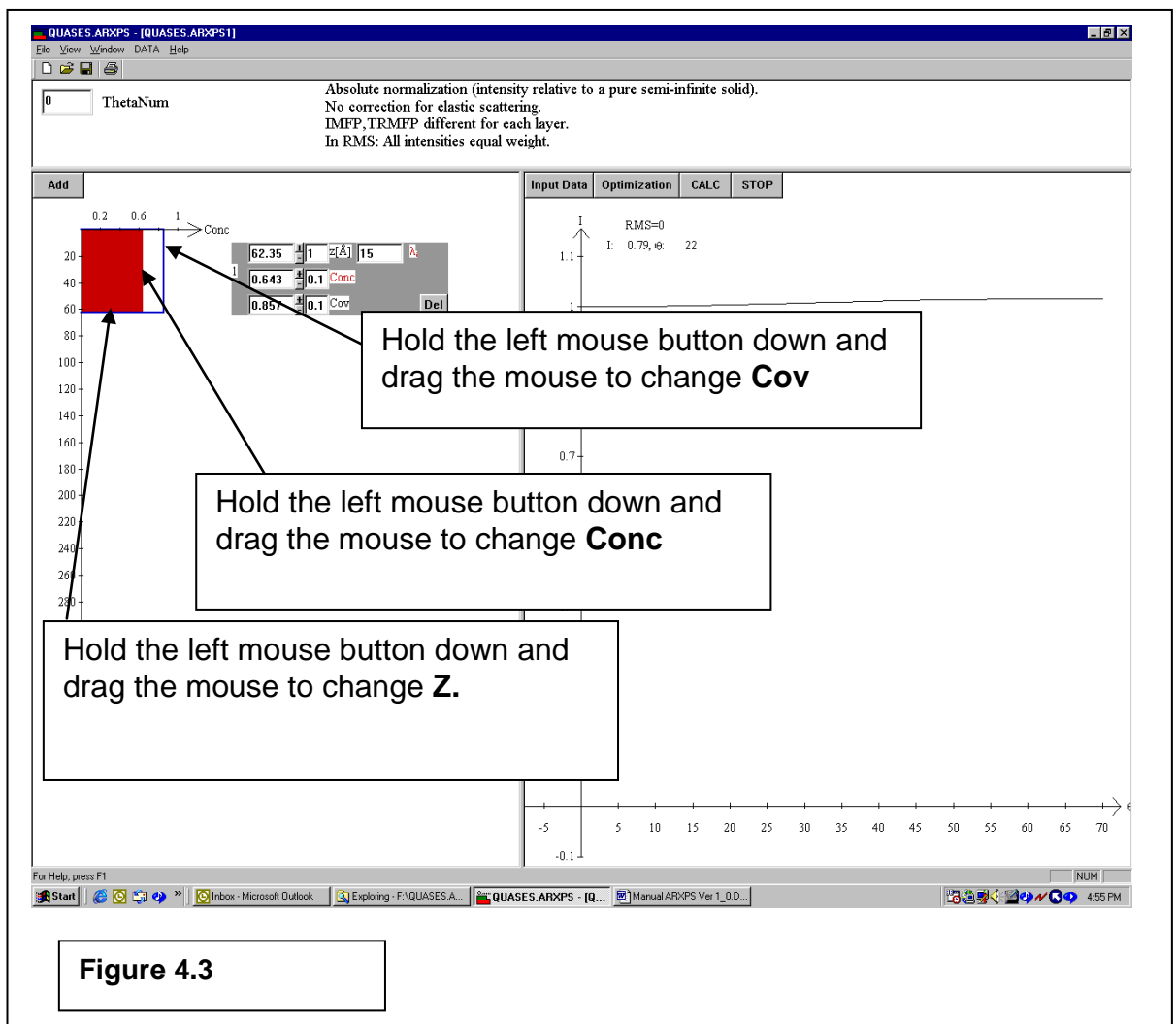
To set the layer thickness measured in Å, click the + or – buttons next to the text box, labeled **Z**, with the layer thickness.

To set the concentration of the material, click the + or – buttons next to the text box, labeled **Conc** with the concentration.

To set the fraction of the surface area that the layer covers, click the + or – buttons next to the text box, labeled **Cov** with the coverage.

The increments when clicking the + or – buttons are set in the text box to the right of the buttons.

Alternatively, the values of **Z**, **Conc**, and **Cov** may be set by holding the left mouse button down and dragging the mouse cursor up and down (to set **Z**) right and left (to set **Cov**) and right and left a second time (to set **Conc**.) (see Figure 4.3).



Click the **ADD** button to add new layers. For each layer, the concentration and coverage can be set as described above (as an example, see Figure 4.4). The layers can be removed by clicking the **Del** button.

For each layer, the inelastic electron mean free path ( $\lambda_i$ ) can be set in the textbox to the left of  $\lambda_i$ . Values for  $\lambda_i$  may be found in [28,29] or they may be calculated by the program QUASES-IMFP-TPP2M™ which is provided with the QUASES-ARXPS™ software package.

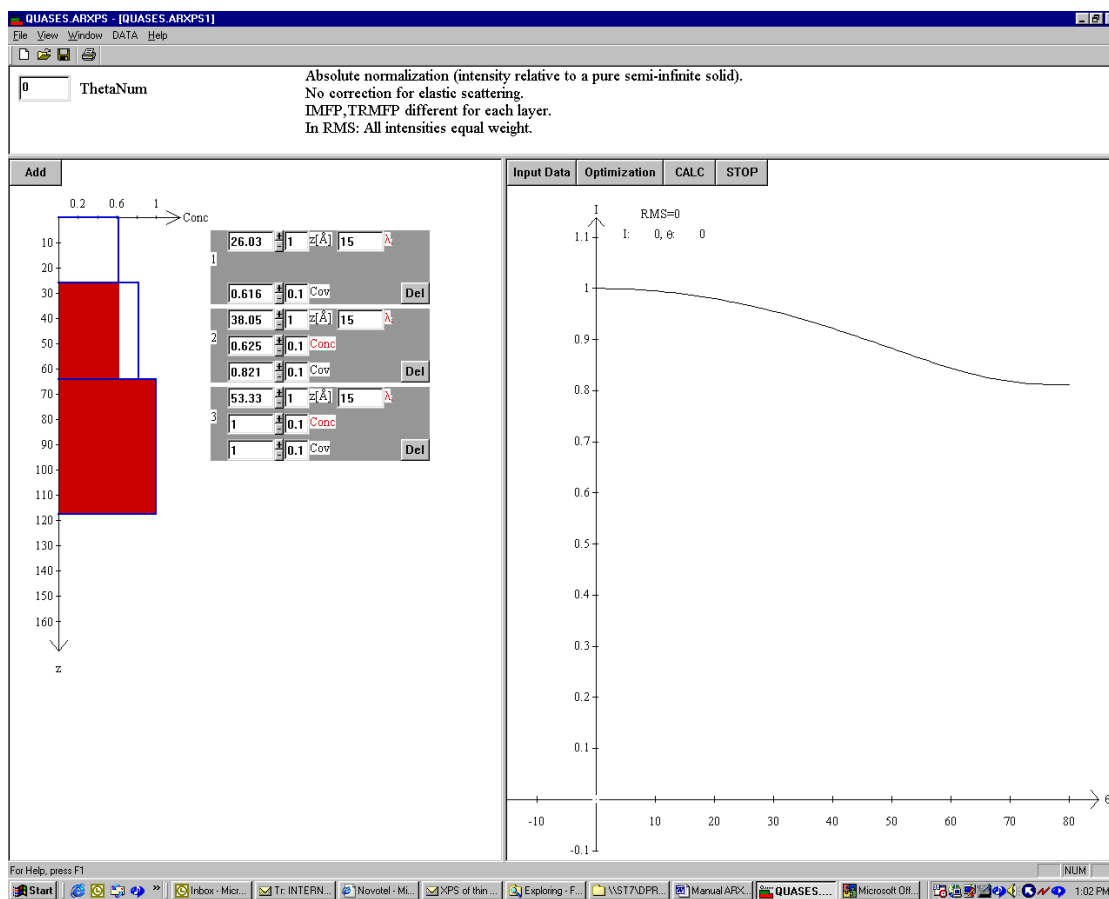
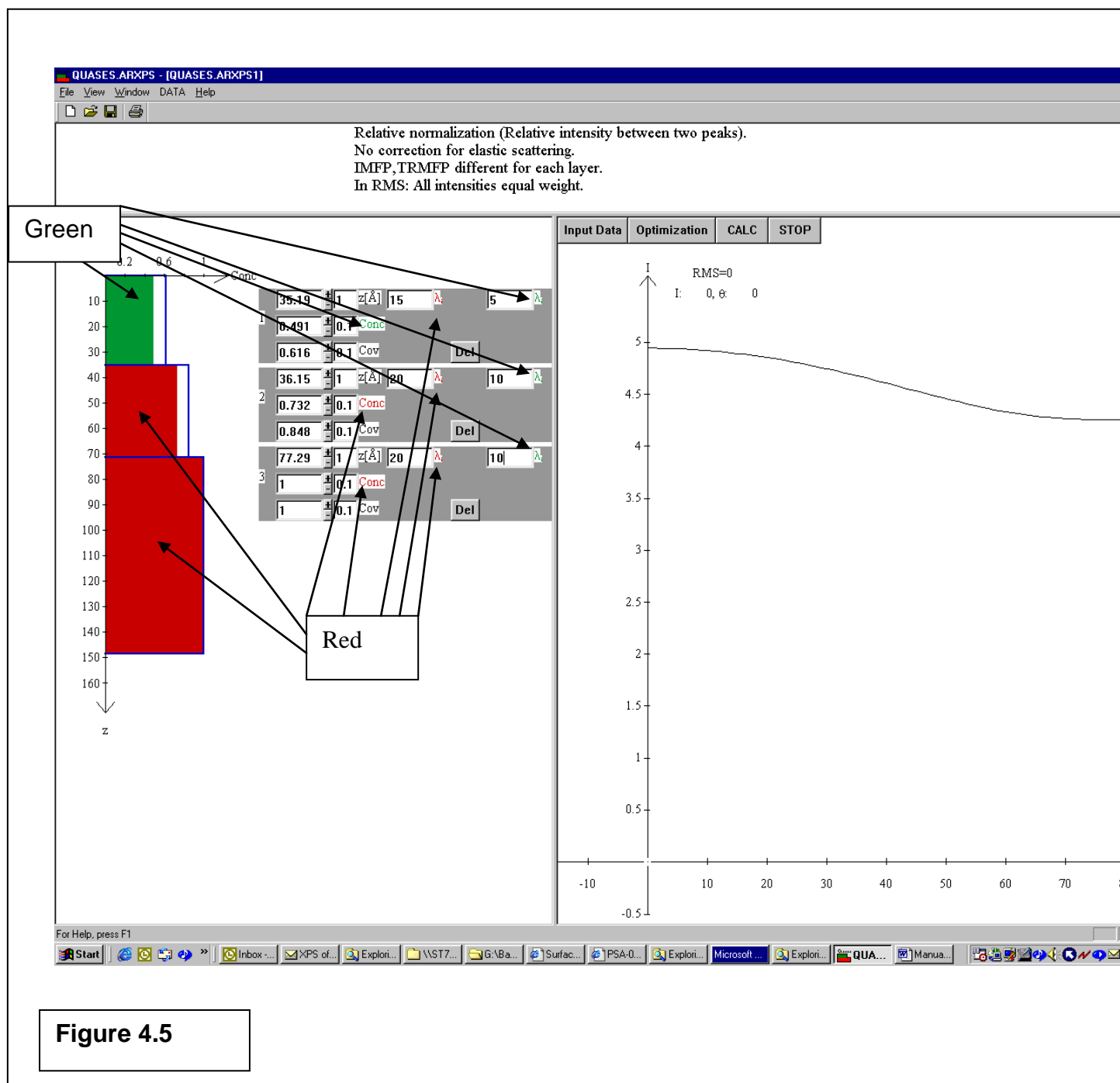


Figure 4.4

When **Relative normalization** is used, there are two photoelectron peaks. This is specified in the following way. The atoms that emit the photoelectrons are marked as “red” and “green” respectively. To activate a layer, place the mouse cursor over the layer and right click once; the layer turns red. Right clicking once more and the layer turns green. Right clicking again and the layer turns inactive. (For an example, see figure 4.5).



The inelastic mean free path (IMFP) for the “red” and “green” electrons are set for each layer. In the example shown in figure 4.5, the IMFP for the “red” electrons is 20 Å in layers 2 and 3, and 15 Å in layer 1, while the IMFP for the “green” electrons is 10 Å in layers 2 and 3, and 5 Å in layer 1.

If **Correction for elastic scattering effect** is set to Yes in the **New Profile Type** dialog box, values for the elastic transport mean free path (TRMFP) are required. The program gives new text boxes where the TRMFP ( $\lambda_{tr}$ ) for each layer and type of electron is input (see figure 4.6).

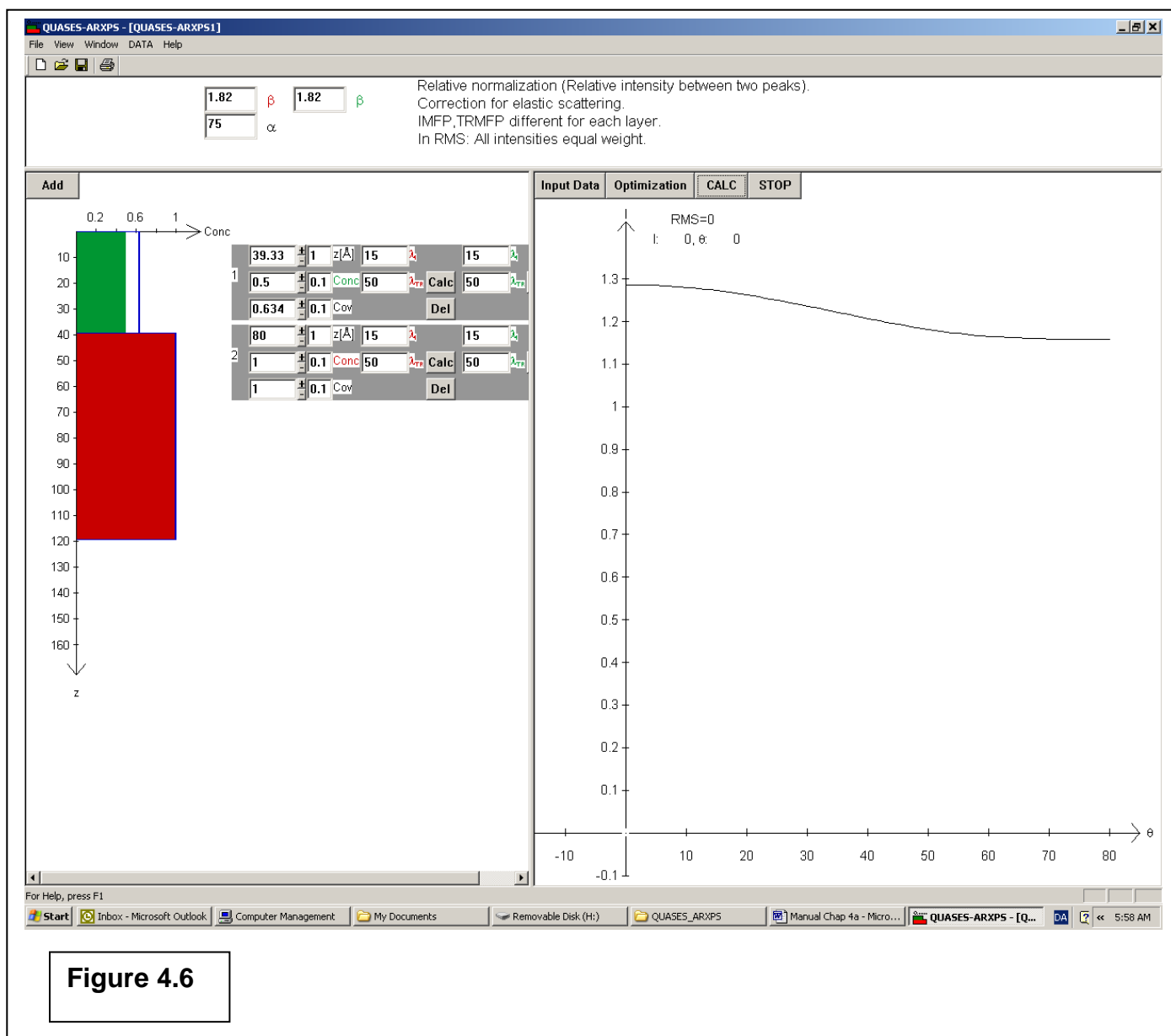
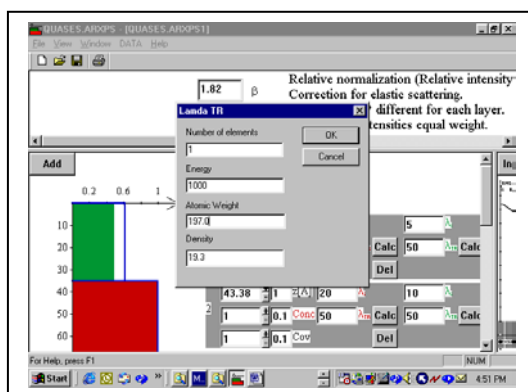
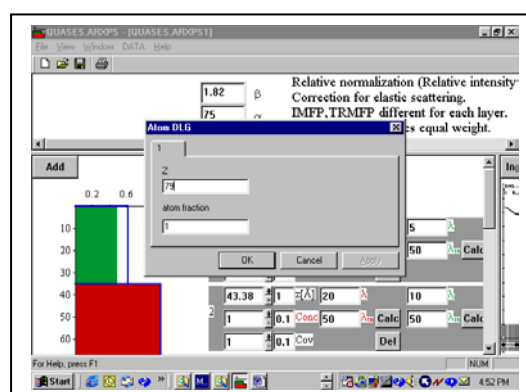


Figure 4.6

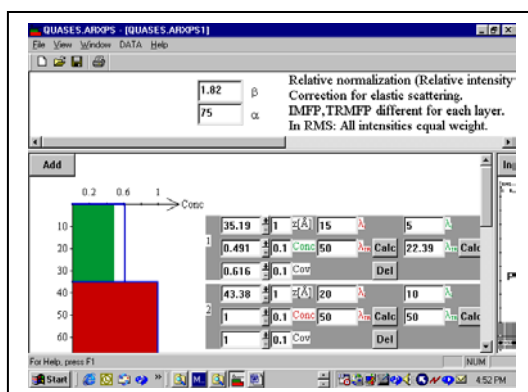
The TRMFP can be calculated by clicking the **Calc** button to the right of  $\lambda_{tr}$  (see figure 4.6). The program uses the algorithm published by Jablonski [30]. Figure 4.7 shows an example where the TRMFP for 1000 eV electrons in gold is calculated.



A



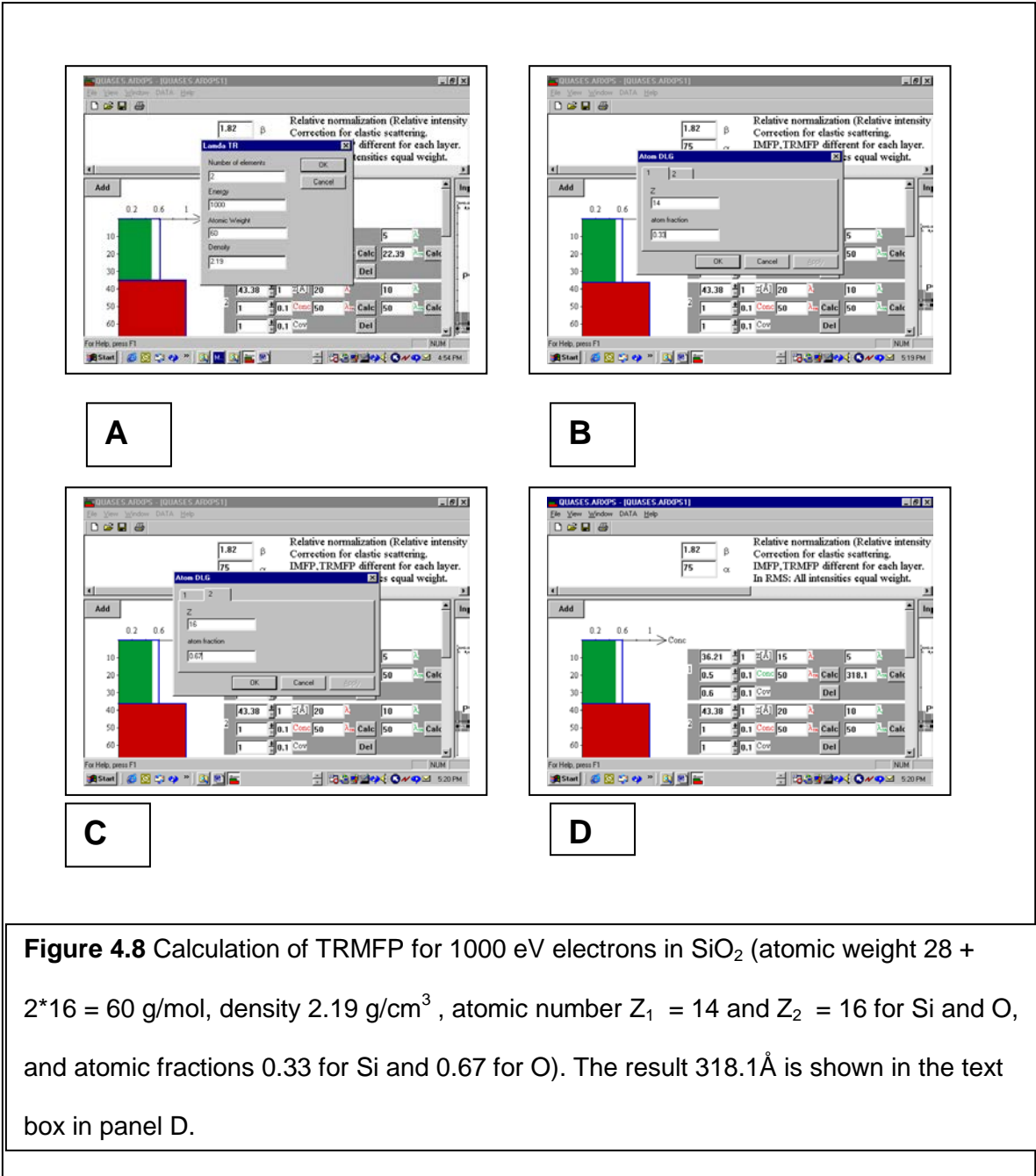
B



C

**Figure 4.7** Calculation of TRMFP for 1000 eV electrons in gold (atomic weight 197 g/mol, density 19.3 g/cm<sup>3</sup>, atomic number Z= 79). The result 22.39Å is shown in the text box in panel C.

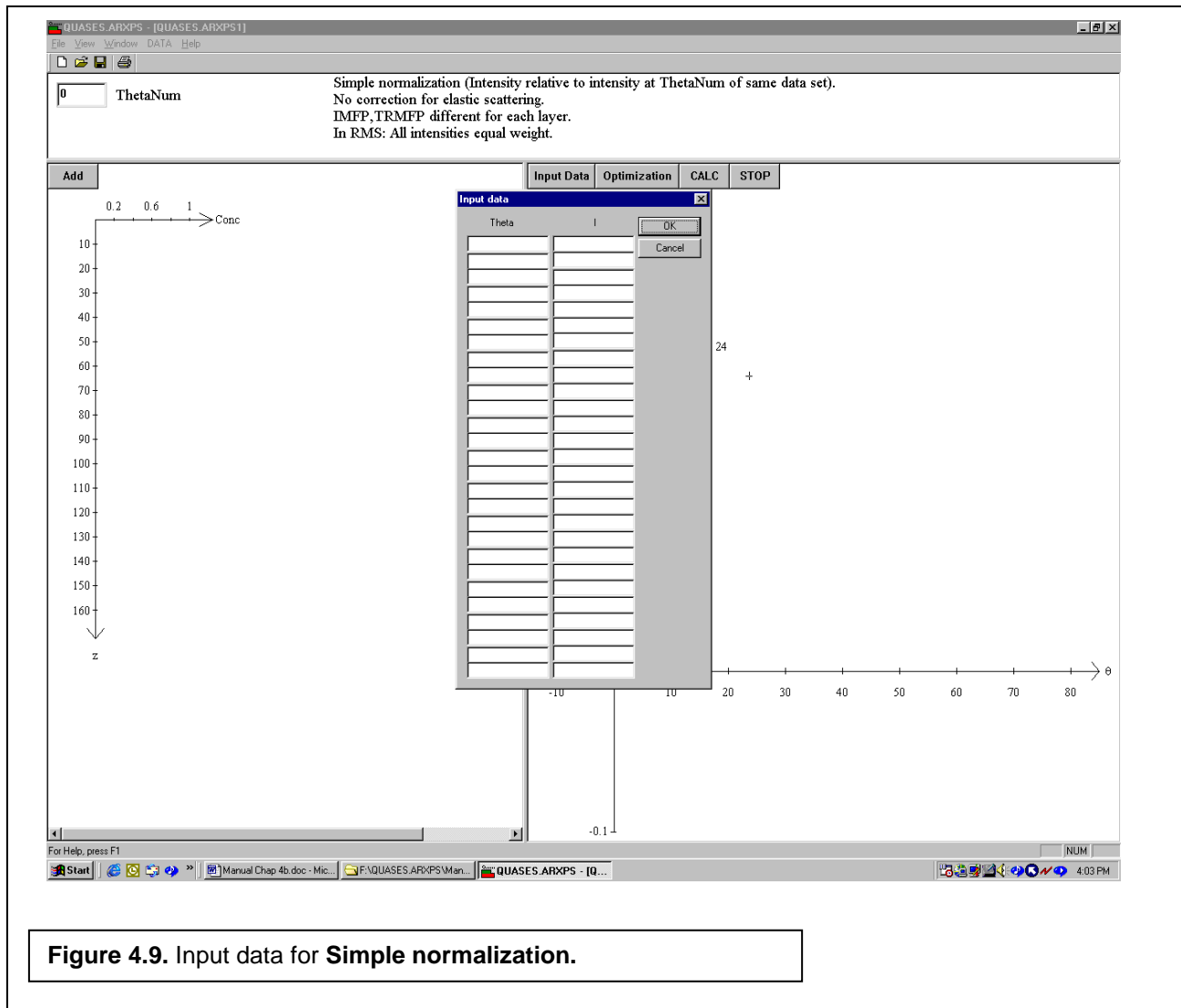
Figure 4.8 shows how this is used to calculate the TRMFP for a compound. SiO<sub>2</sub> is taken as an example.



## 4.4 Data-frame

### 4.4.1 Input Data

To input experimental intensities, click **Input Data** and get figure 4.9 for **Simple normalization**, figure 4.10 for **Absolute normalization** and figure 4.11 for **Relative normalization**.



For **Simple normalization** (figure 4.9) the first row is the angle of emission with respect to the surface normal and the second row is the measured peak intensity.

For **Absolute normalization** (figure 4.10) the first row is the angle of emission with respect to the surface normal, the second row is the measured peak intensity and the third row is the measured peak intensity from a pure infinite sample.

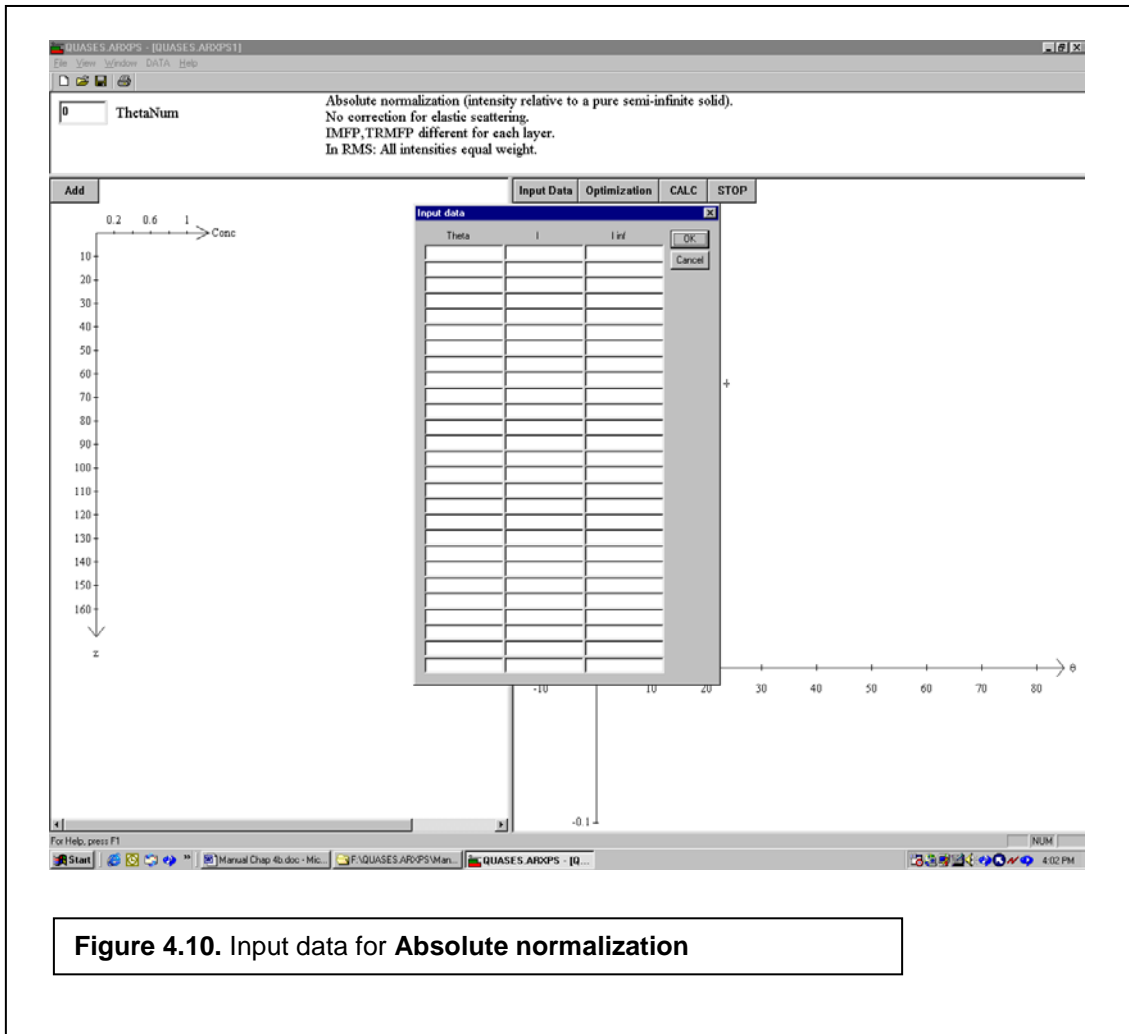


**Figure 4.10.** Input data for **Absolute normalization**



## 4.4.2 Optimization

Click the *Optimization* button to optimize the agreement between experimental and theoretical peak intensities. This gives figure 4.12. In the dialog box, there is a tab for each layer. Under each tab, all parameters can be selected. The program will look for an optimal solution (lowest RMS deviation from the experimental data) by changing the values of all ticked parameters between the values given in Min and Max text boxes. In the example shown, only the height of layer 1 will be optimized within values  $0 \leq Z \leq 300$  while the concentration, the coverage and the IMFP are kept constant at the values set in the **Profile-frame**.

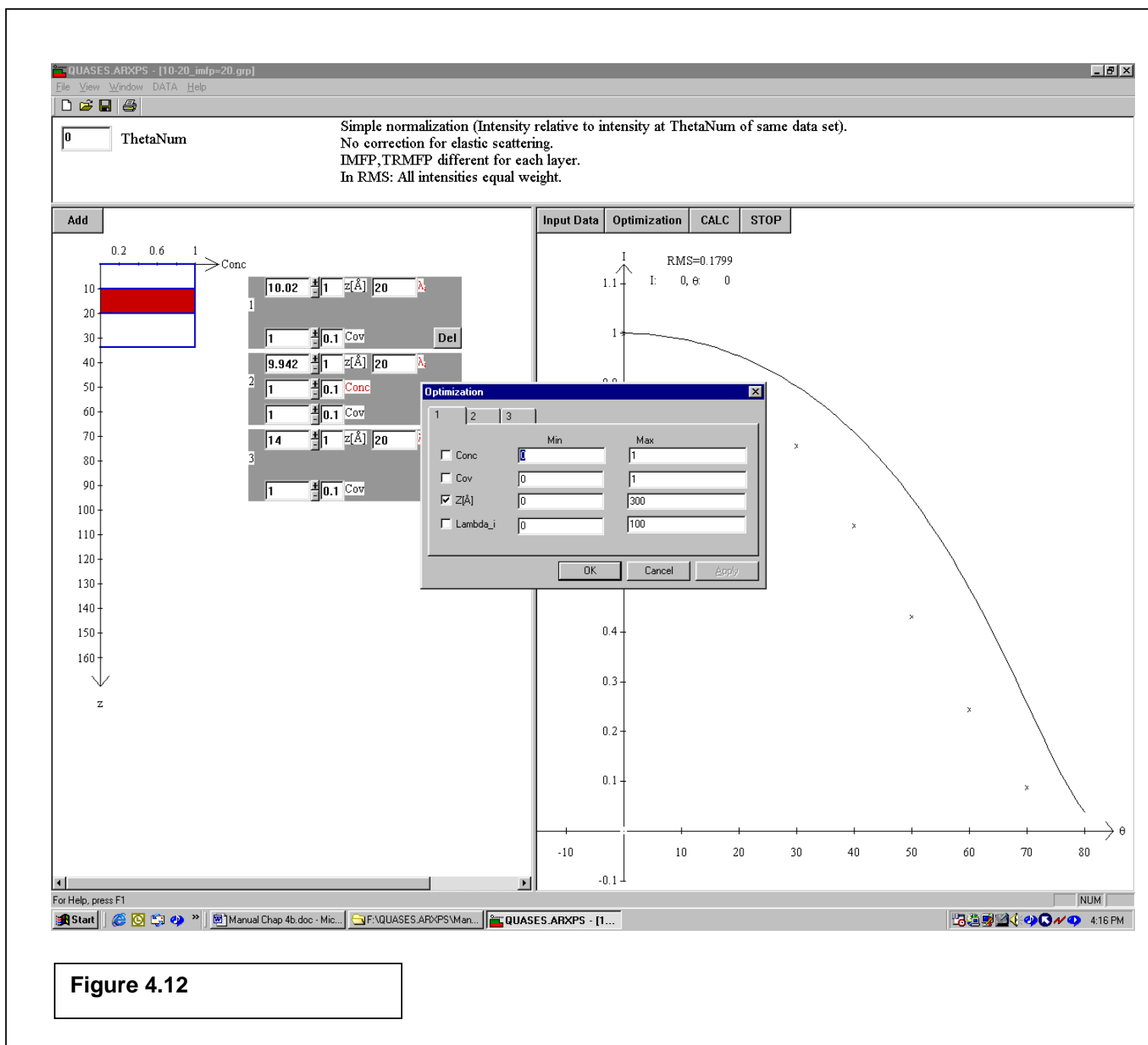


Figure 4.12

**Calc**

The *Calc* button is used to force the calculations to be updated. This is mainly used when elastic scattering correction is applied because the calculation time is longer.

**Stop**

The *Stop* button stops the calculations.

## 4.5 Menu Bar

To get the **Setup** dialogue box, click **File** and then click **Setup** (see figures 4.13 and 4.14).

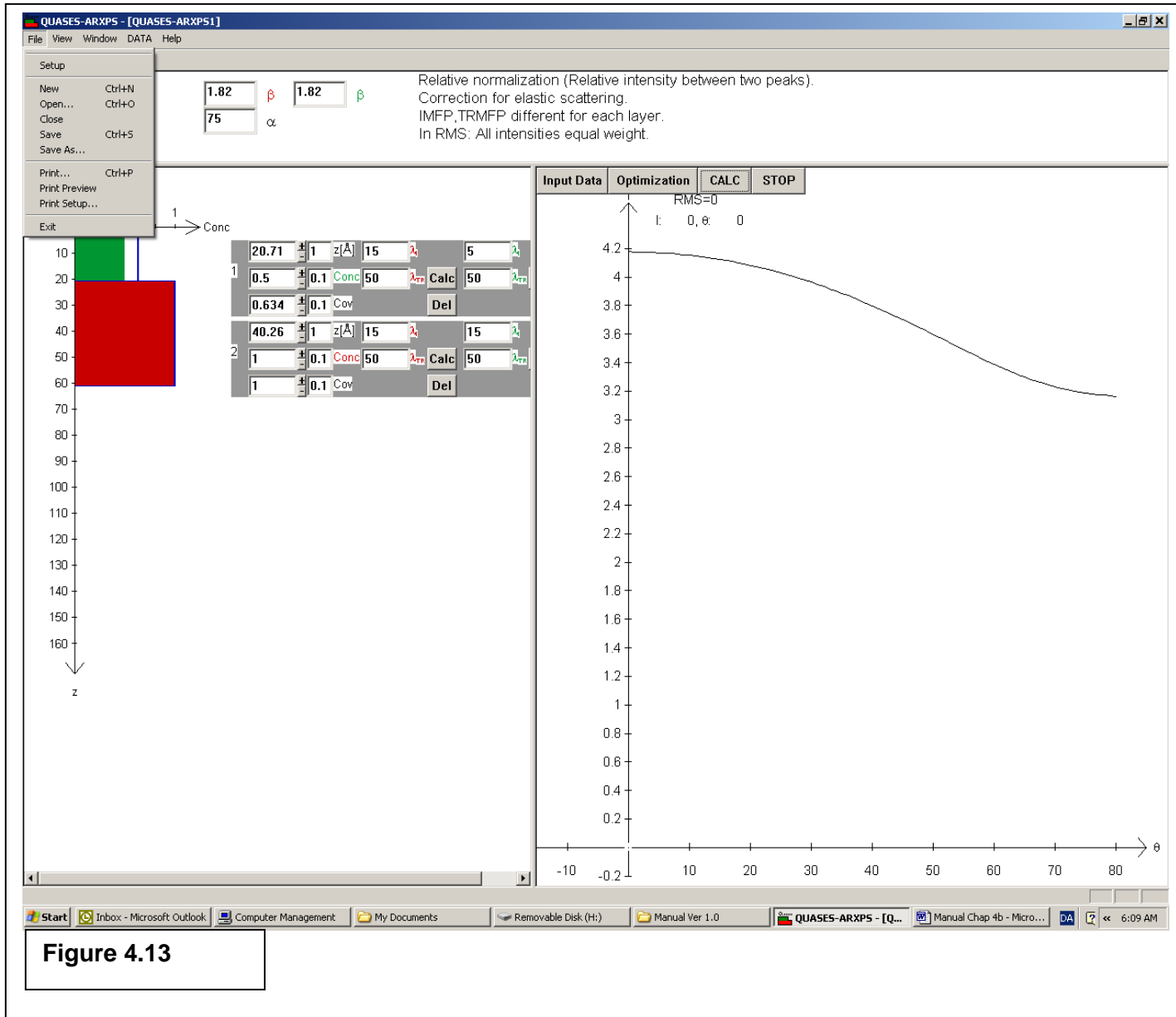


**Figure 4.13**

In the dialog box, 6 parameters can be set:

**Max depth:** This is the maximum depth shown in the plot in the **Profile-frame**.

**Theta step size:** The size of steps in  $\theta$  in the calculations shown in the **Data-frame**.

**Theta max:** The maximum  $\theta$  used in the calculations shown in the **Data-frame**.

**Internal data path:** The working directory of the program. If it is blank, the working directory is the same as the directory where the program was started.

**Tol:** Used to control the accuracy of all calculations in the program (typical value  $0.00001 < \text{Tol} < 0.001$ ). Smaller value gives longer computation time.

**Min RMS for optimization:** Used to control the stop criterion in the Simplex and Powell optimization procedures. The optimization stops when the RMS (eq. (3.19) or (3.20)) gets below this value.

**Number of Steps:** This is used only in the simple optimization method (see below).

**Optimization method:**

- **Simple:** Makes a grid where each parameter to be optimized is varied between the Min and Max values (this is set in the **Optimization** dialog box in **Data-frame**). The distance between the points in the grid is  $(\text{“Max”}-\text{“Min”})/\text{“Number of steps”}$  for each parameter. Calculates RMS deviation for each point in the grid and returns the lowest point. This method is slow but gives a global minimum provided that the Number of steps is sufficiently large.
- **Simplex:** Uses the Simplex method [31] to find the set of parameters with the lowest RMS value.
- **Powell:** Uses the Powell method [32] to find the set of parameters with the lowest RMS value.

Note that the Simplex [31] and Powell [32] methods have here been modified in order to handle finite parameter intervals.

It is generally recommended to use the Simplex algorithm (best compromise between accuracy and speed).

The rest of the menu items are standard Windows dialogues for file- and print-handling.

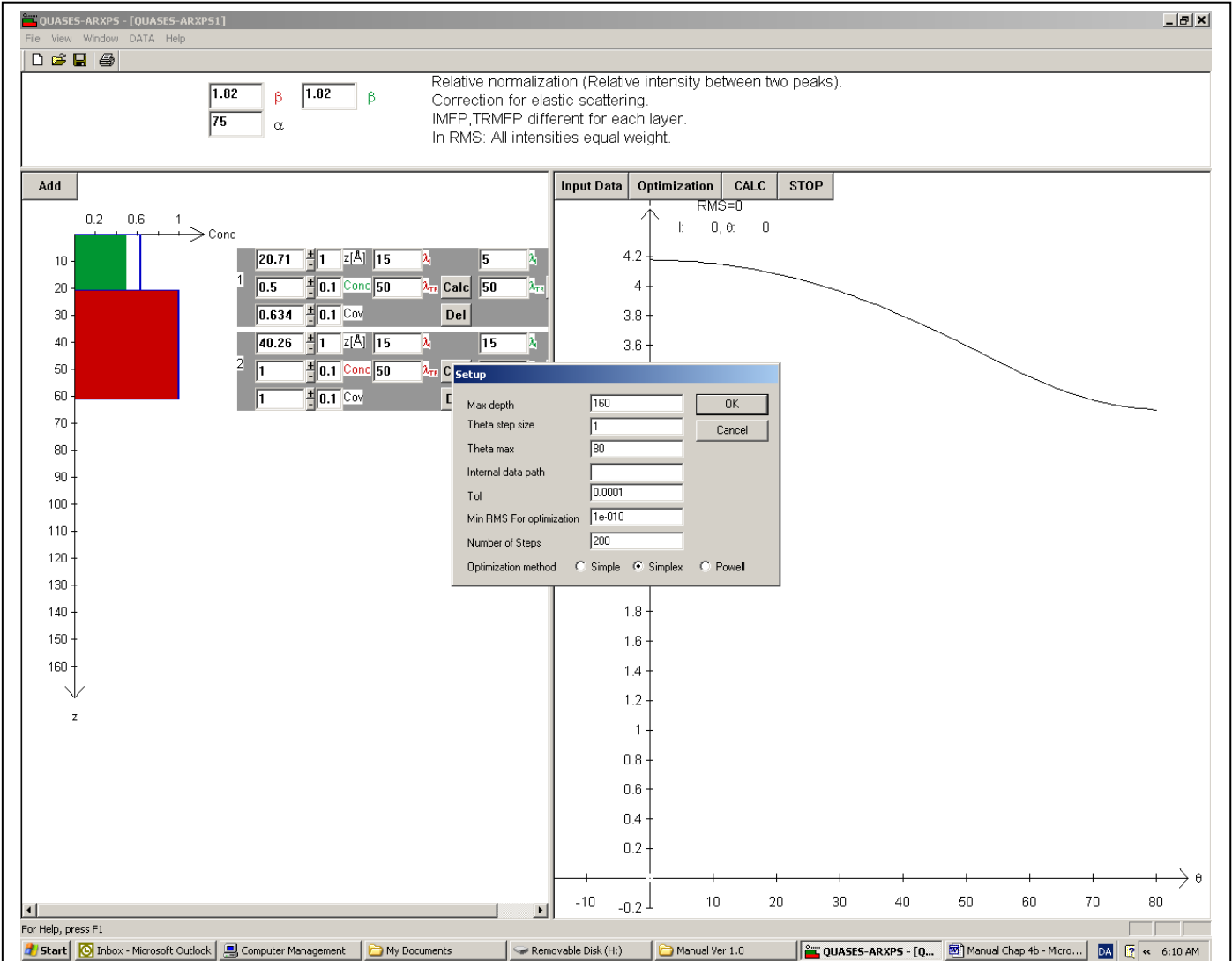


Figure 4.14

# Chapter 5

## File formats

### 5.1 Save

It is possible to save the data in 3 different file formats.  
Click File + Save As to get figure 5.1

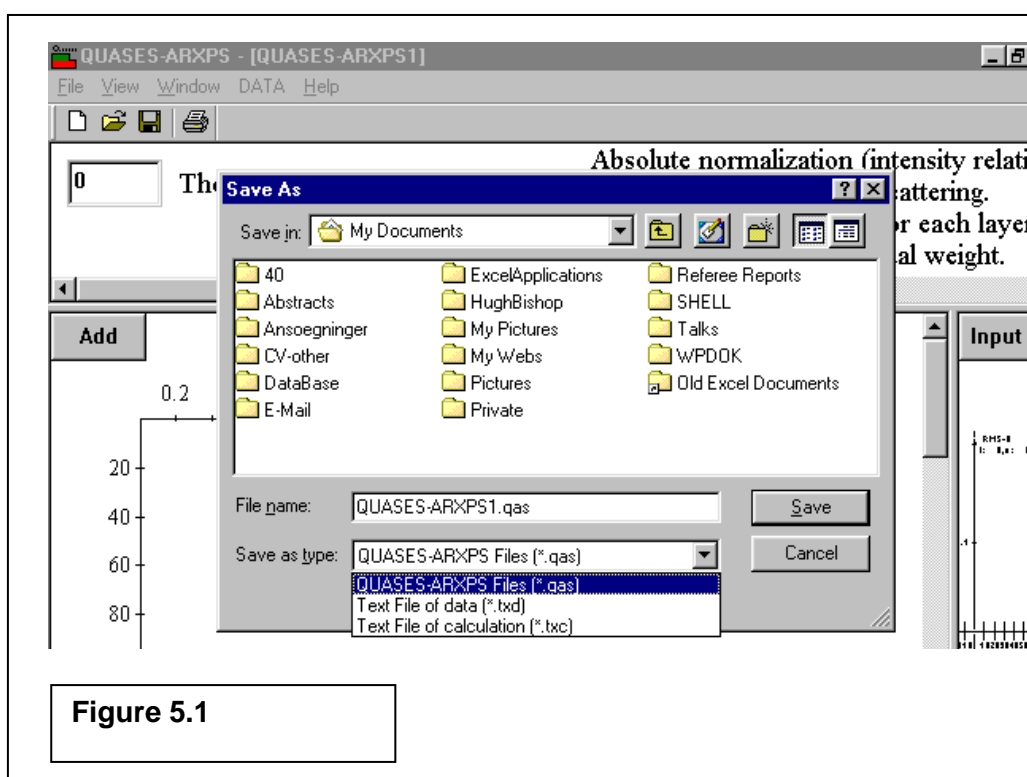


Figure 5.1

**QUASES-ARXPS Files (\*.qas):** binary data format. All information saved.

**Text File of data (\*.txd):** ASCII-text format of normalized experimental data points.

**Text File of calculation (\*.txc):** ASCII-text format of normalized calculated data points.

The binary data format (\*.qas) is used to store the present status of the analysis. The ASCII-text formats (\*.txd) and (\*.txc) are used to store the calculated and experimental data points for import in a another program (e.g. a spreadsheet).

## 5.2 Open

It is possible to open files with data in 4 different formats.  
Click File + Open to get figure 5.2

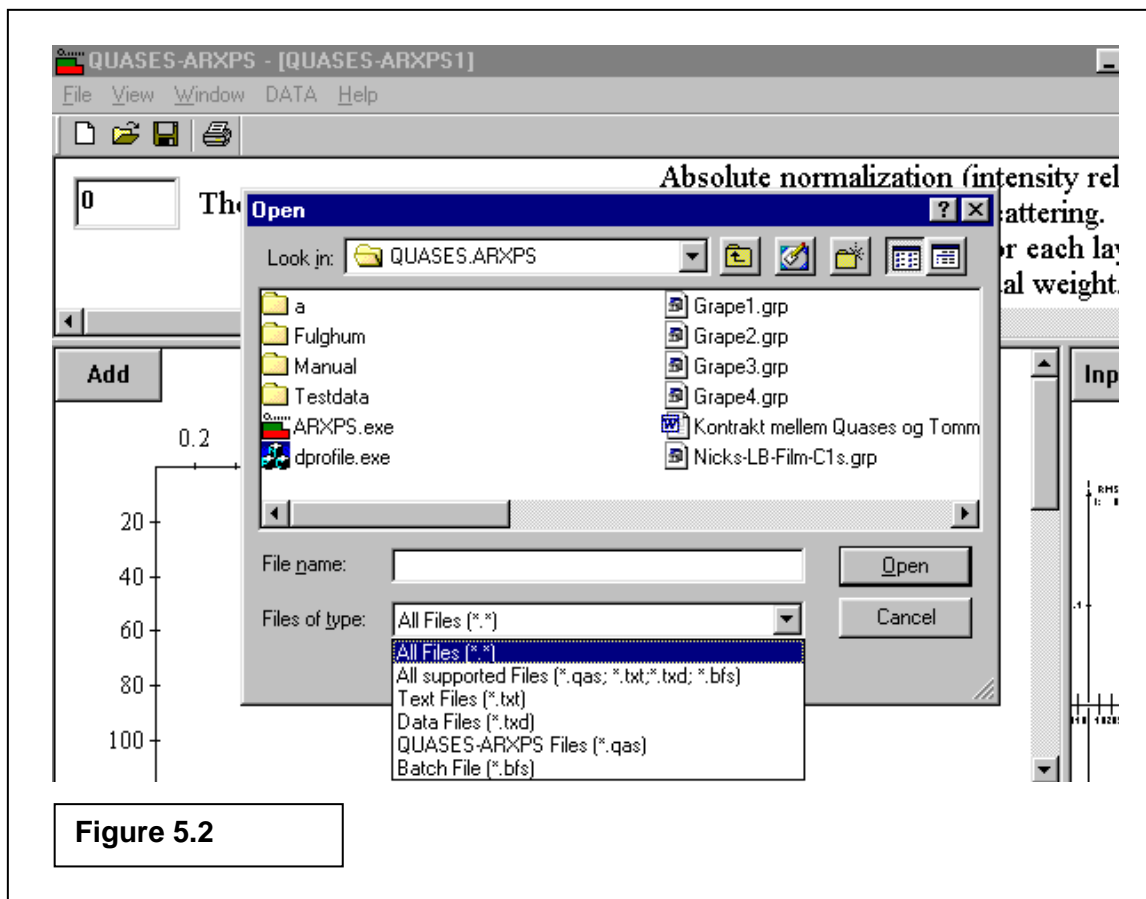


Figure 5.2

**QUASES-ARXPS Files (\*.qas):** binary data format. All information loaded.

**Text Files (\*.txt):** ASCII-text format used only internally. Not recommended.

**Data Files (\*.txd):** ASCII-text format of experimental data points (2 and 3 columns, comma separated).

**Batch File (\*.bfs):** ASCII-text format used only internally. Not recommended.

The binary data format (\*.qas) is used to load the previous status of the analysis. The ASCII-text formats (\*.txd) is used to load the experimental data points (e.g. from a spreadsheet). If the file contains two columns these are read as (angle, intensity). If the data file contains three columns, the data are read as (angle, intensity, intensity Inf) when absolute normalization is used and as (angle, intensity A, intensity B) when relative normalization is used.

**Don't use the (\*.txt) and (\*.bfs) data formats.**

# Chapter 6

## Tutorials

### 6.1 Simple normalization

Click **Data** on the menu bar. Select **Simple normalization** and click **OK**. Then click **Input Data** in the **Data-frame** and get the **Input data** dialog box. Input the data in table 6.1 in the **Input data** box (see figure 6.1). Then click **OK**.

Theta	I
0	6.32
10	6.38
20	6.55
30	6.85
40	7.29
50	7.89
60	8.65
70	9.46

Table 6.1

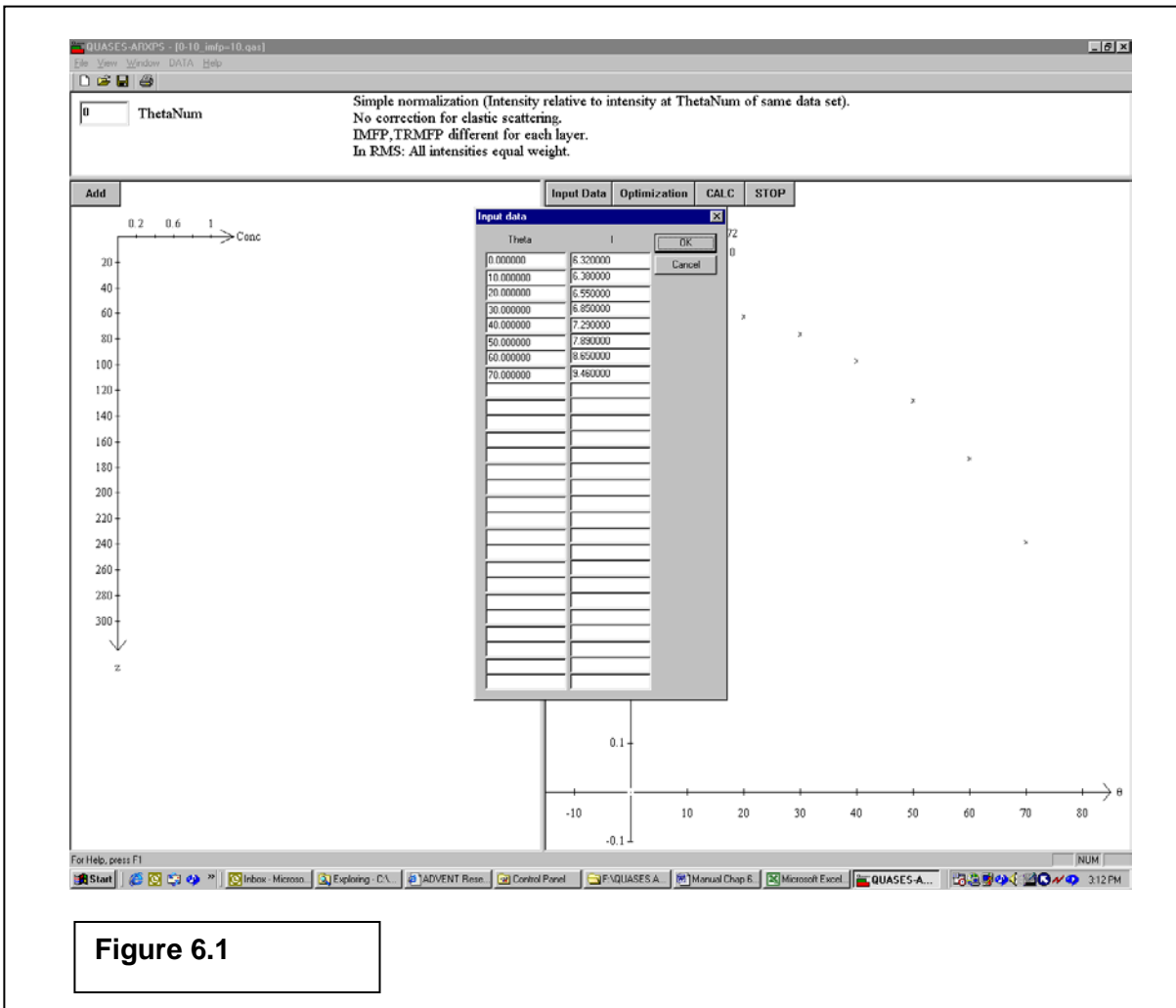
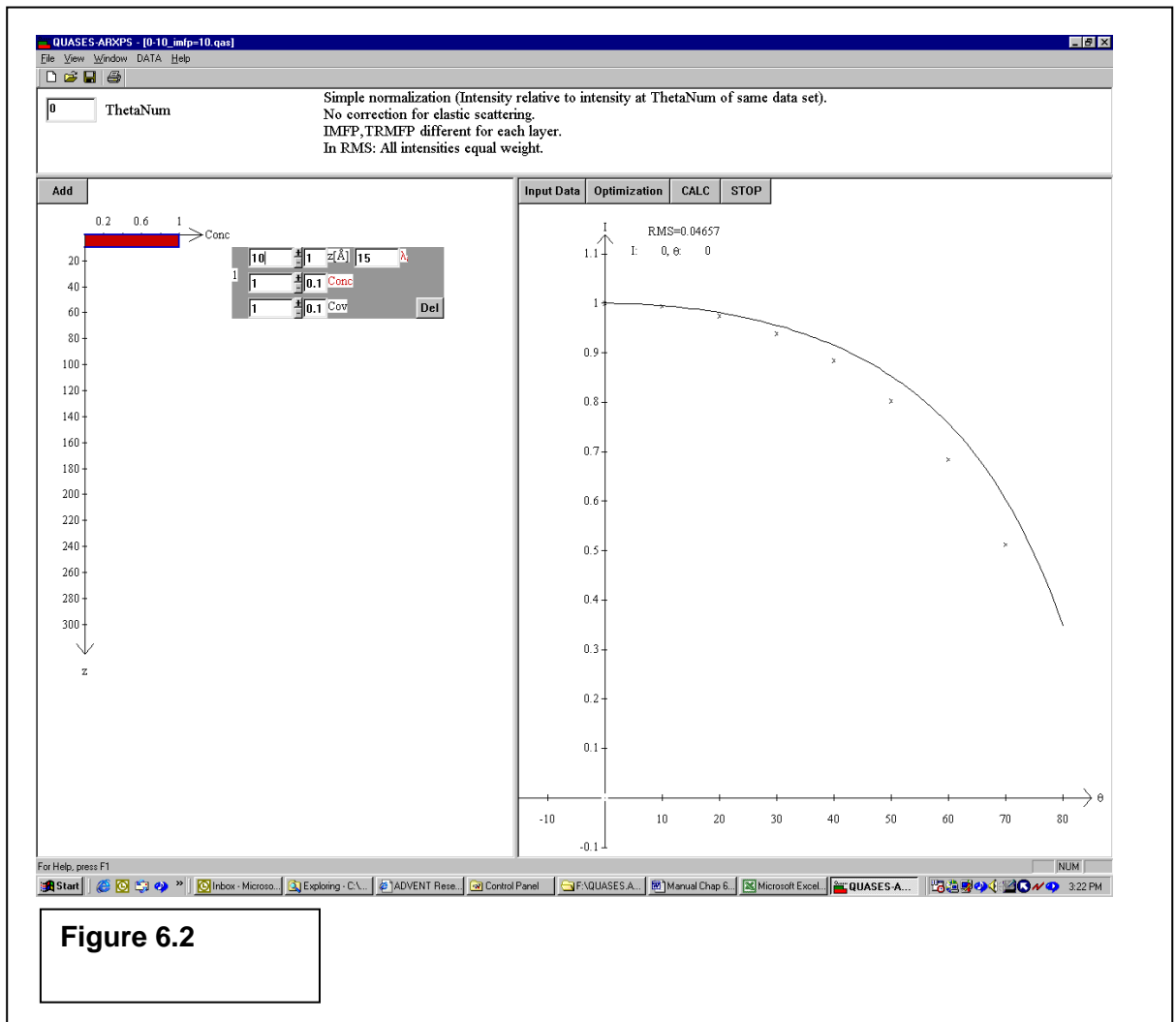


Figure 6.1

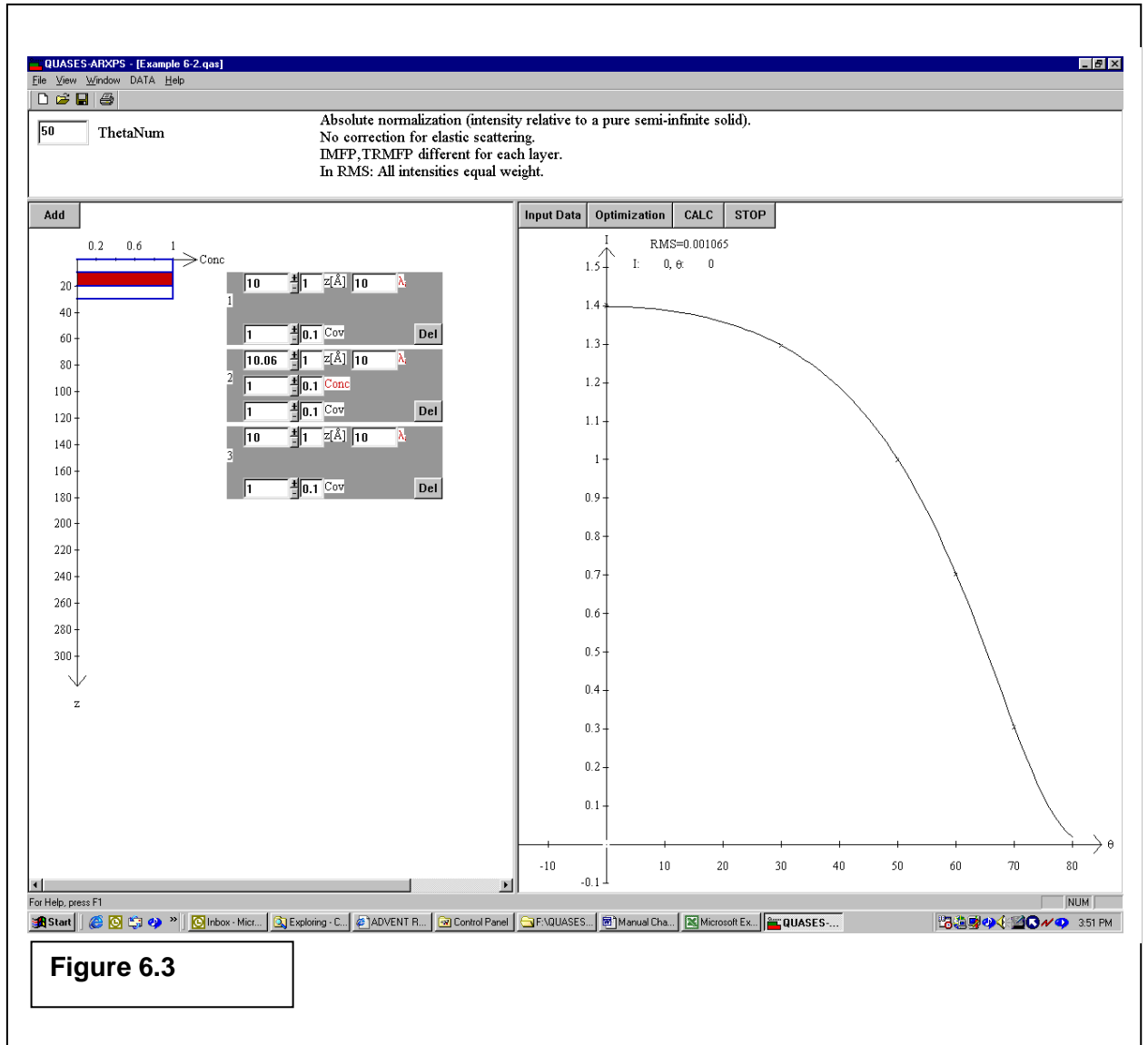
Click **Add** in the **Profile-frame**, then activate the layer by placing the mouse cursor over the layer and right click and get figure 6.2. The graph displayed in the **Data-frame** shows the experimental data points as “x” and the solid line is the theoretical curve. The data set in table 6.1 was constructed for an IMFP = 10 Å. Change  $\lambda_i$  to 10 Å to get a perfect fit between theory and experiment in the graph displayed in the **Data-frame**.



**Figure 6.2**

## 6.2 Absolute normalization

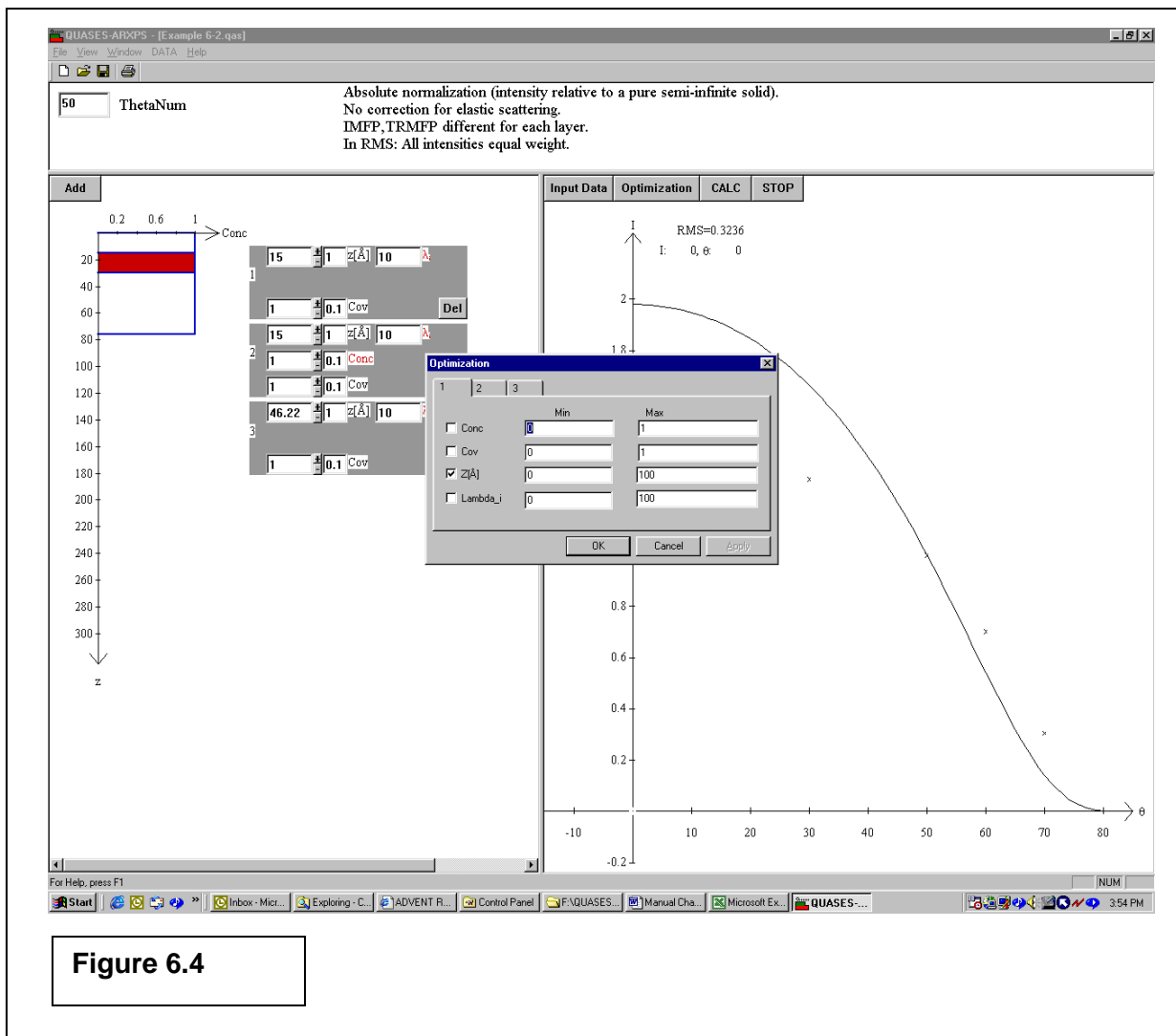
Click **File**, then click **Open** and select the file “Example 6-2.qas” from the file list box, click the **Open** button and get figure 6.3.



Change the **Z** value for layer 3 and notice that the calculated curve does not change. This is because no emitted electrons pass through this layer.

Now change the **Z** values for layers 1 and 2 to  $Z = 15 \text{ \AA}$ . Notice the disagreement between theory and experiment.

Then click **Optimization** in the **Data-frame** and get figure 6.4. Tick the Check box for **Z** for layers 1 and 2 and make sure that no other Check boxes are ticked. Click **OK**. This produces a perfect fit with the new optimized thicknesses shown in the **Profile-frame**.



### 6.3 Relative normalization

Click **File**, then click **Open** and select the file “Example 6-3.txd” from the file list box, click the **Open** button.

Then Click **Data** on the menu bar and select **Relative normalization** and click **OK**. Then you get figure 6.5.

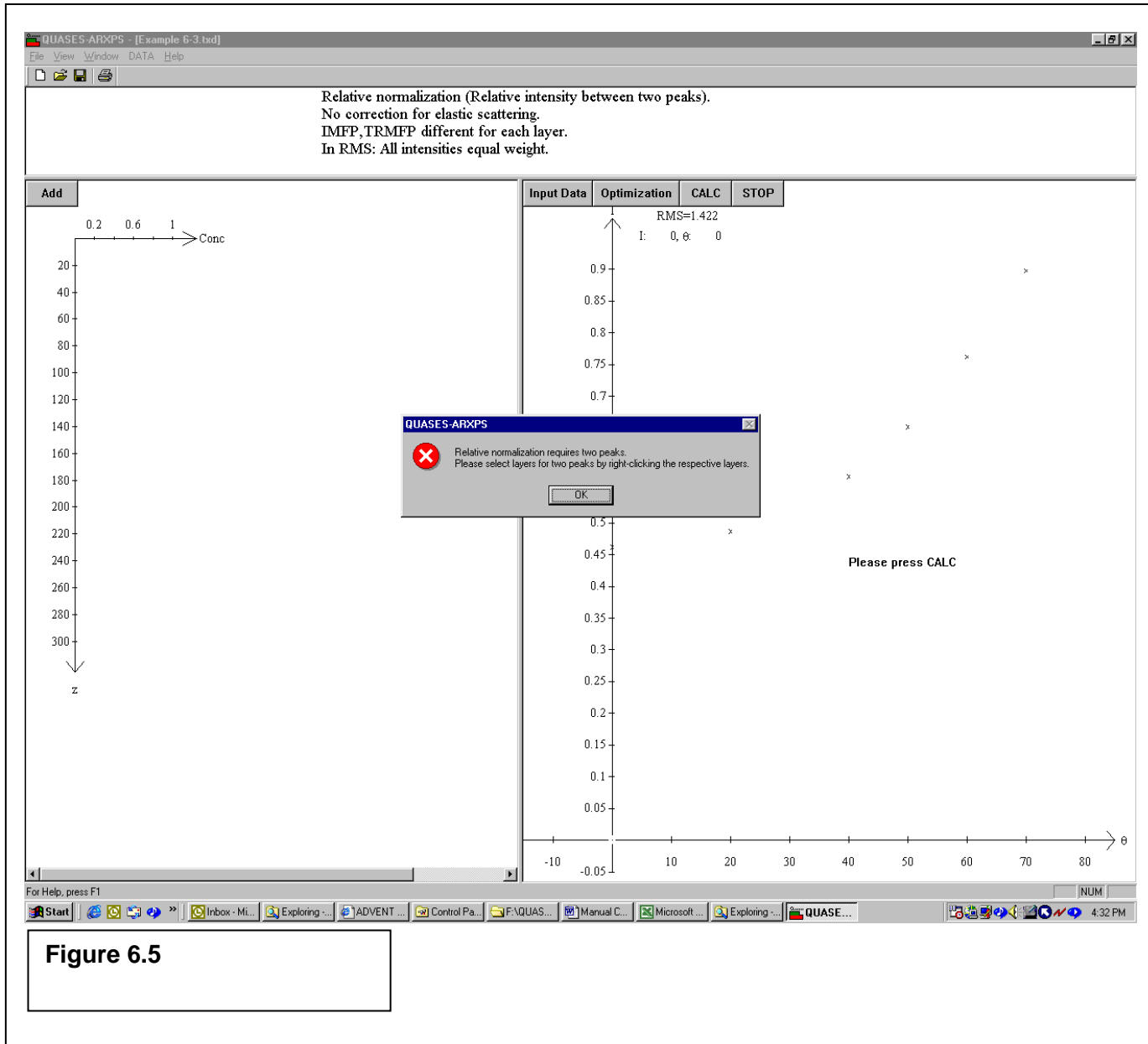


Figure 6.5

Note the warning, which tells that two peaks are required when relative normalization is used. Click **OK** to remove the warning box. Then click the **Add** button twice to create two layers in the Profile-frame. Activate layer 1 as “green” atoms by placing the mouse cursor over the layer and right click twice. Activate layer 2 as “red” atoms by placing the mouse cursor over the layer and right click once. This produces figure 6.6.

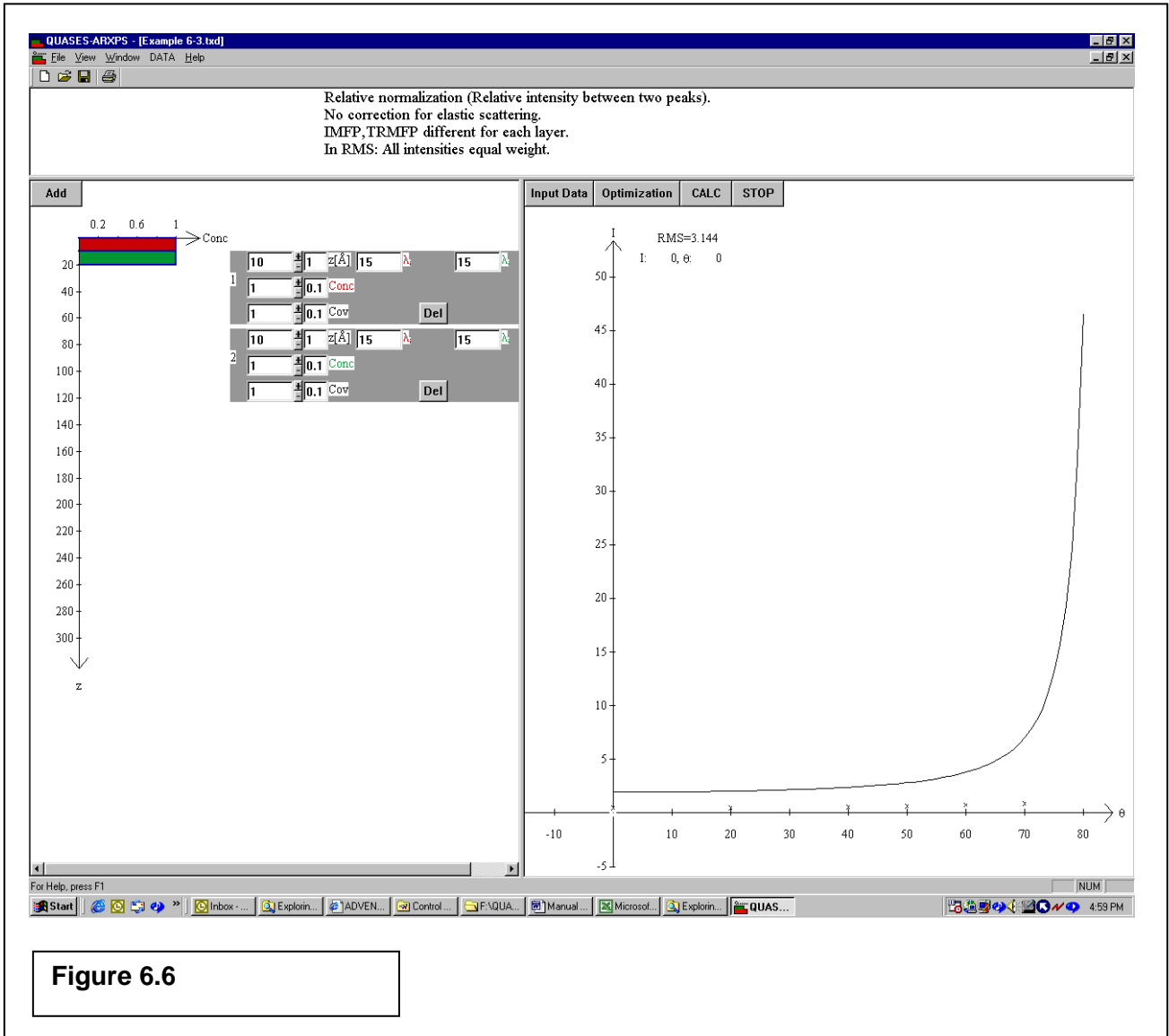
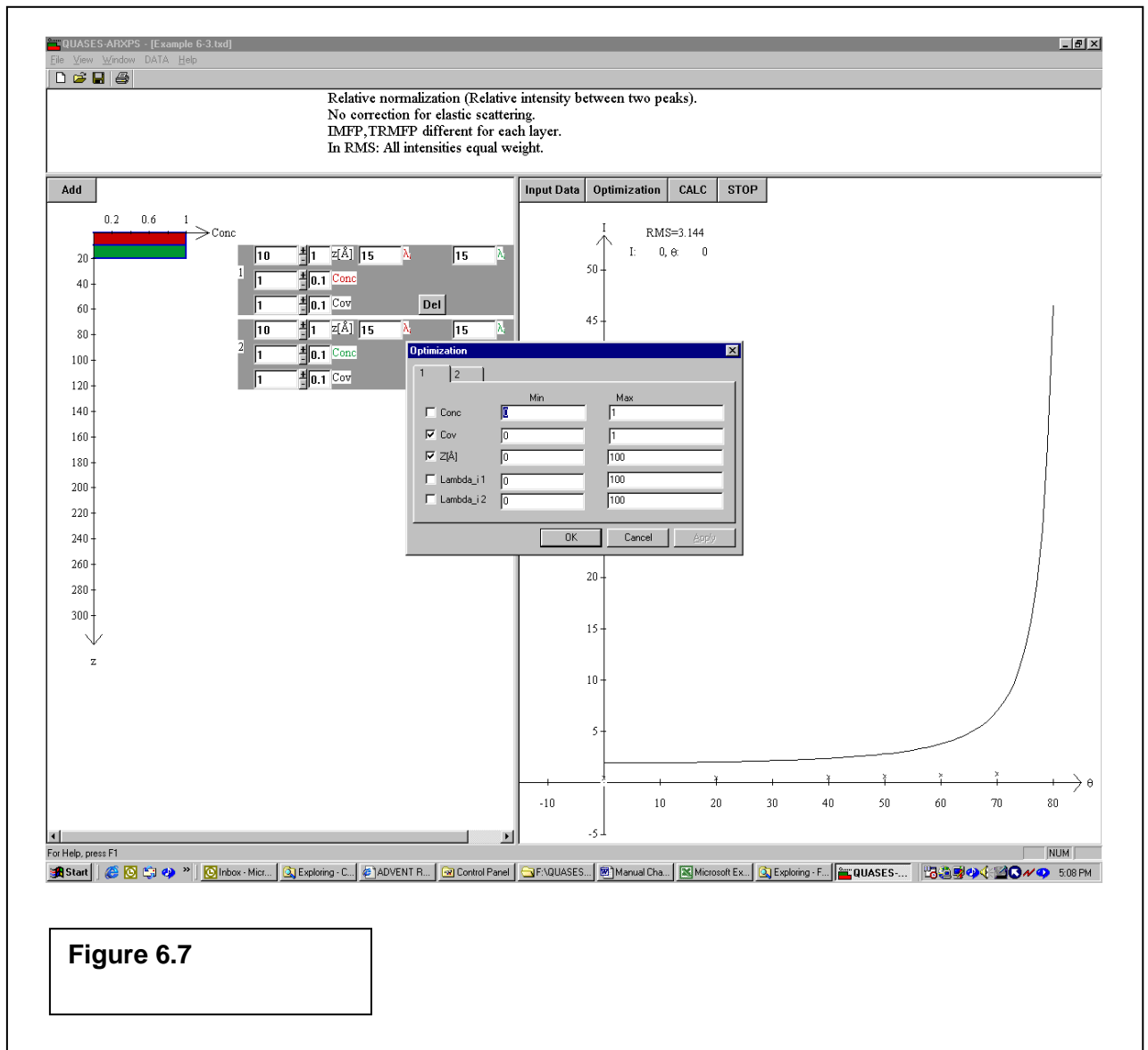
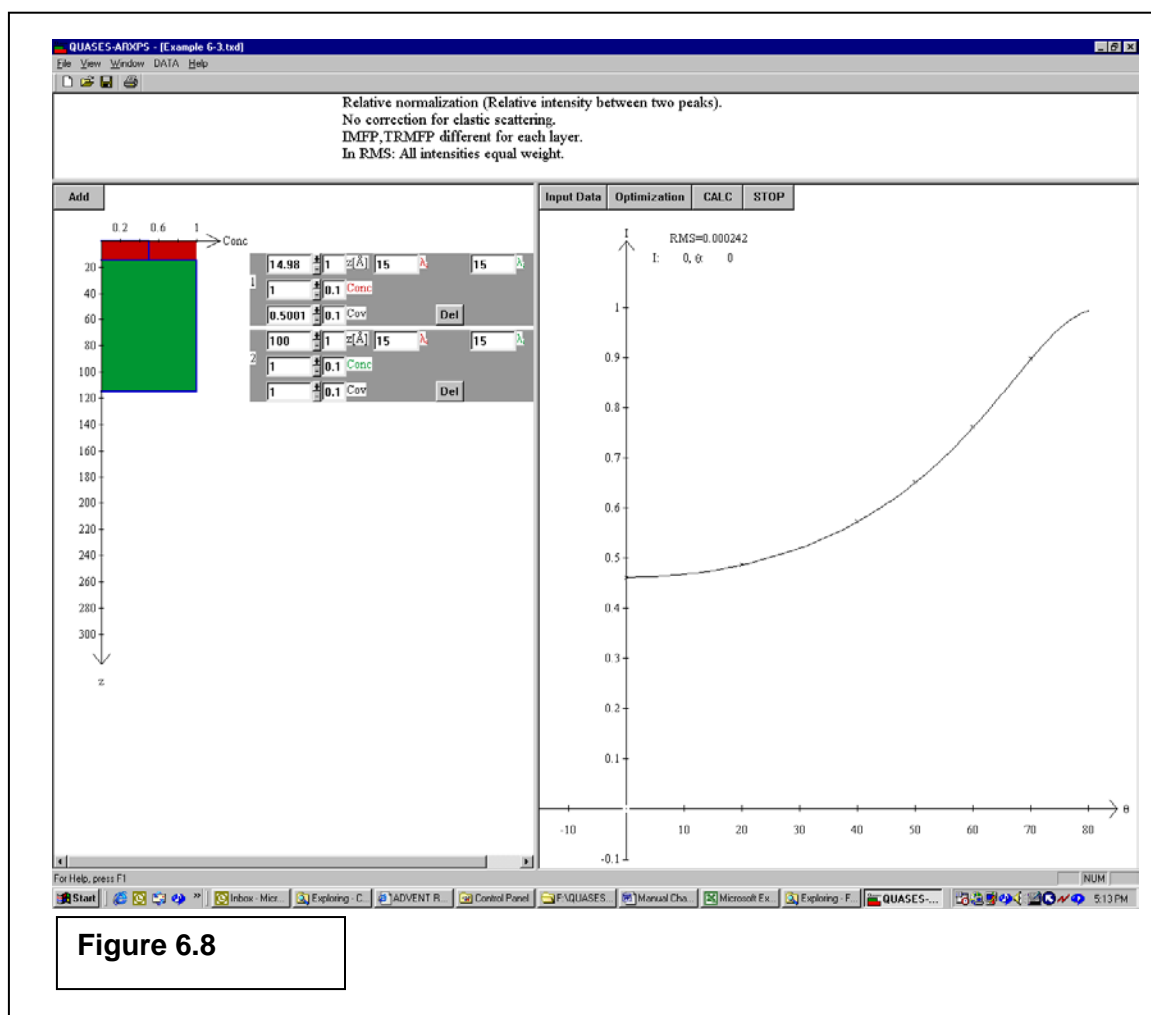


Figure 6.6

Click the **Optimization** button in the **Data-frame**. Tick the check boxes for **Z** and **Cov** for layer 1 and **Z** for layer 2 and make sure that no other check boxes are ticked. Click **OK** and get the perfect fit in figure 6.8.

The parameters for the optimized fit are shown in the Profile-frame. This shows that the sample consists of two layers where layer 2 consists of “green” atoms of height 100 Å and with concentration = 100 % and coverage = 100 % and layer 1 consists of “red” atoms of height 15 Å and with concentration = 100 % and coverage = 50 %.





## 6.4 Elastic scattering

Click **File** then click **Open** and select the file “Example 6-2.qas” to open the data from section 6.2 Click the **Del** button in layer 3 to remove the layer.

Click the **Data** menu item + **New Profile Type** and click the **Yes** button in the **Correction for elastic scattering effects** group. Click **OK**. Click the **Calc** button in the **Data-frame** and see that the calculated curve has changed (see figure 6.9). This change is due to elastic electron scattering which is determined by  $\lambda_{tr}$  which is set to 50 Å for both layers. Increase the  $\lambda_{tr}$  value for both layers to 500 Å. Click the **Calc** button and see that the effect of elastic electron scattering is now much smaller.

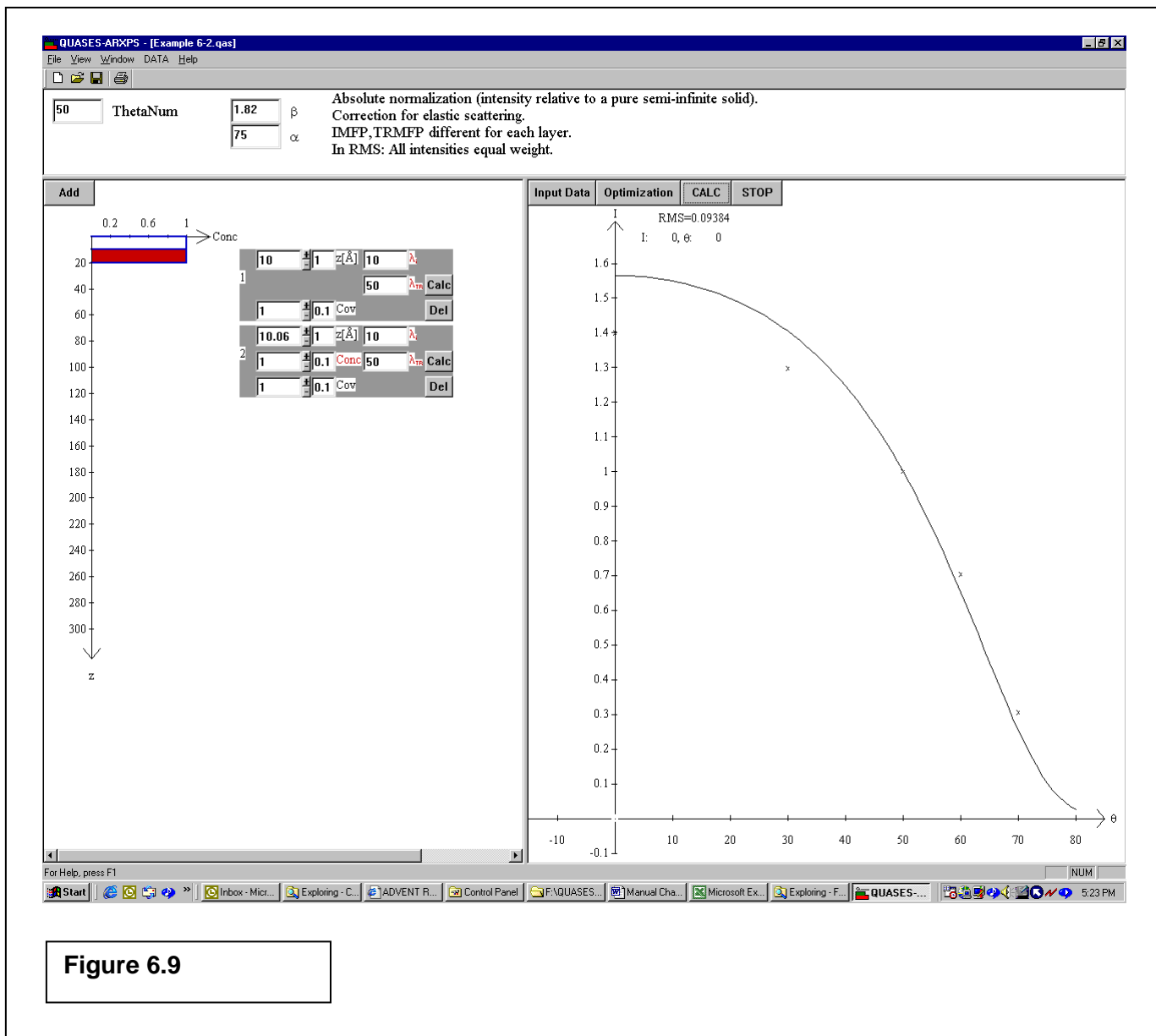


Figure 6.9

## References

- [1] S. Tougaard, *J. Vac. Sci. Technol.* A5 (1987) 1230
- [2] S. Tougaard, *Applied Surf. Sci.*, 32 (1988) 332
- [3] S. Tougaard, *J. Vac. Sci. Technol.* A8 (1990) 2197
- [4] S. Tougaard, *Surf. Interf. Anal.* 26 (1998) 249
- [5] C. S. Fadley, R. J. Baird, W. Siekhaus, T. Novakov, and S. Å. L. Bergström, *J. Electr. Spectr.* 4 (1974) 93
- [6] P. H. Holloway, *J. Vac. Sci. Technol.* 12 (1975) 1418.
- [7] O. A. Baschenko and V. I. Nefedov, *J. Electron Spectrosc. Relat. Phenom.* 27 (1982) 109.
- [8] M. F. Ebel, *J. Electron Spectrosc. Relat. Phenom.* 22 (1981) 157.
- [9] H. Ebel, M. F. Ebel, J. Wernisch and A. Jablonski, *J. Electron Spectrosc. Relat. Phenom.* 34 (1984) 355.
- [10] T. D. Bussing and P. H. Holloway, *J. Vac. Sci. Technol.* A3 (1985) 1973.
- [11] J. E. Fulghum, *Surface Interface Anal.* 20 (1993) 161.
- [12] P. J. Cumpson, *J. Electron Spectrosc. Relat. Phenom.* 73 (1995) 25.
- [13] I. S. Tilinin, A. Jablonski and W. S. M. Werner, *Progress Surface Sci.* 53 (1996) 193.
- [14] V. I. Nefedov, *J. Electron Spectrosc. Relat. Phenom.* 100 (1999) 1
- [15] W. S. M. Werner, G. C. Smith and A. K. Livesey, *Surface Interface Anal.* 21 (1994) 38.
- [16] A. Jablonski and S. Tougaard, *Surface Sci.* 432 (1999) 211.
- [17] T. S. Lassen, S. Tougaard and A. Jablonski, *Surface Science* 481(2001)150

- [18] W. S. M. Werner, W. H. Gries and H. Störi, Surf. Interface Anal. 17 (1991) 693
- [19] W. S. M. Werner and I. S. Tilinin, Surface Sci. 268 (1992) L 319
- [20] W. S. Werner, Surface Interface Anal. 20 (1993) 727
- [21] A. Jablonski and S. Tougaard, Surface Interface Anal. 26 (1998) 17
- [22] A. Jablonski and S. Tougaard, Surface Interface Anal. 26 (1998) 374
- [23] V. I. Nefedov and I. S. Fedorova, J. Electron Spectrosc. Relat. Phenom. 85 (1997) 221
- [24] I. S. Tilinin, A. Jablonski, J. Zemek and S. Huaeck, J. Electron Spectrosc. Relat. Phenom. 87 (1997) 127
- [25] P. J. Cumpson and M. P. Seah, Surf. Interf. Anal. 25 (1997) 430
- [26] W. A. M. Aarnik, A. Weishaupt, and A. Silfhout. Applied Surf. Sci. 45 (1990)37
- [27] M. Band, Yu. I. Kharitonov and M. B. Trzhaskovskaya, At. Data Nucl. Data Tables 23 (1979) 443
- [28] S. Tanuma, C.J. Powell, D. R. Penn, Surf. Interf. Anal. 21(1994) 195
- [29] C. J. Powell and A. Jablonski, J. of Physical and Chemical Reference Data, 28 (1999) 19
- [30] A. Jablonski, Phys. Rev. B58 (1998) 16470
- [31] W. H. Press, W. T. Vetterling, S. A. Teukolski, and B. P. Flannery in *Numerical recipes in FORTRAN the art of scientific computing*, Chapter 10, pages 402-406. Cambridge University Press, Second edition, 1992
- [32] W. H. Press, W. T. Vetterling, S. A. Teukolski, and B. P. Flannery in *Numerical recipes in FORTRAN the art of scientific computing*, Chapter 10, pages 390-398, 406-413. Cambridge University Press, Second edition, 1992

**QUASES-ARXPS**